

# The SIS process on Erdős-Rényi graphs: determining the infected fraction

O.S. Awolude<sup>1</sup>, E. Cator<sup>1</sup>, and H. Don<sup>1</sup>

<sup>1</sup>*Department of Mathematics, Radboud University, Heyendaalseweg  
135, Nijmegen, 6525 AJ, Gelderland, Netherlands*

July 12, 2024

## Abstract

There are many methods to estimate the quasi-stationary infected fraction of the SIS process on (random) graphs. A challenge is to adequately incorporate correlations, which is especially important in sparse graphs. Methods typically are either significantly biased in sparse graphs, or computationally very demanding already for small network sizes. In this paper we present a new method to determine the infected fraction in sparse graphs, which we test on Erdős-Rényi graphs. Our method does take into account correlations and gives accurate predictions. At the same time, computations are very feasible and can easily be done even for large networks.

**Keywords:** SIS process, Erdős-Rényi graph, Metastable behaviour, Infected fraction

## 1 Introduction

The Covid-19 virus was first identified in Wuhan (China) in December 2019, when it started to spread very quickly worldwide. In this initial stage, the number of cases was growing exponentially fast and the disease was disrupting society. In the next few years, many people got infected and there were several peaks of infections of the virus and its variants. Right now, it seems the situation is stabilizing. A large part of the world population has been infected at least once and many people have built up immunity. The number of new cases has dropped, but the disease still goes around and is expected to stay forever. The World Health Organization (WHO) shifts its focus from emergency response to long term Covid-19 disease management [25]. In this paper, we show how to predict and explain the behaviour of infectious diseases after stabilization.

Mathematical models for infectious diseases have been studied over the last decades, with a recently boosted interest due to the Covid-19 outbreak. In this

work we focus on the SIS process (or contact process) on finite graphs. In this Markovian model, individuals are represented by nodes in a graph, which are either healthy or infected. Each infected node heals at rate 1, and it infects each of its healthy neighbors at rate  $\tau$ . This means that healthy individuals are always susceptible to the disease, like in the endemic Covid-19 phase. It motivates the terminology susceptible-infected-susceptible (SIS). For more background on the SIS process and related models, we refer to [21, 20], [8].

The SIS process was first introduced by Harris [16] in 1974. Harris studied the process on the integer lattice  $\mathbb{Z}^d$ . It has later been studied on many other graphs [19, 22, 6, 28, 29], with recent attention to the process on random graphs [2, 4, 17, 23, 24]. Random graphs are designed to model social interactions within populations, and as such are suitable to model a population in which an infectious disease is spreading. Our focus in this paper is on the SIS process on Erdős-Rényi random graphs [11, 14]. For background on random graphs in general and the Erdős-Rényi graph in particular, we refer to [12, 3, 30].

A key characteristic of the SIS model on the Erdős-Rényi graph (and many other graphs) is the existence of an epidemic threshold. Below this threshold, the infection dies out exponentially fast. Above the epidemic threshold, extinction only happens at a very large time scale, see [4, 10, 13]. On finite graphs, ultimately the process will reach the only stable solution in which all individuals are healthy. However, before extinction, the process will be in a *metastable* or *quasi-stationary* state, which is quickly reached and corresponds to the Covid-19 endemic phase. Our primary goal in this paper is to get a better understanding of this stabilized behaviour of the SIS-process on sparse graphs, for which the Erdős-Rényi graph is our main test case. We are particularly aiming at determining the infected fraction of the population in the metastable state based on the parameters of the process and on graph characteristics.

## 1.1 Review of models for the infected fraction

Exact analysis of the SIS process and its metastable state is hard, and only few rigorous results are available, even for quite simple graphs [6]. For a general graph given by its adjacency matrix, the probability distribution on the state space can in principle be computed numerically at any time. However, due to the exponential size of the state space, these matrix computations are limited to very small populations.

This is the reason that a lot of attention has gone to methods for approximating the behaviour of the process, see [26] for a discussion of the different approaches. Kephart and White consider the process on regular graphs, and derive a differential equation for the evolution of the infected fraction [18]. Wang et al. [32] had the interesting idea to generalize this to graphs with arbitrary adjacency matrix, but their results were shown to be inaccurate in the metastable regime [31]. This inspired Van Mieghem et al. [31] to introduce the  $N$ -intertwined Mean Field Approximation (NIMFA), which requires solving a system with ‘only’  $n$  unknowns to approximate the metastable infected fraction ( $n$  being the population size). As the authors note, NIMFA overestimates the

metastable infected fraction because it ignores correlations between nodes. As we will see, this is especially problematic if degrees in the graph are small.

The Heterogeneous Mean Field approximation (HMF) in [27] also ignores correlations. In fact, for graphs with exponentially decaying degree distributions (like the Erdős-Rényi graph), [27] proposes to ignore fluctuations in the degree and just use the average. This is the *homogeneous* mean field approximation. Although this is reasonable if the degrees are not too small, it leads to inaccurate predictions for sparse Erdős-Rényi graphs. HMF is proposed in [27] for scale-free graphs, i.e. graphs in which the degree distribution decays polynomially. HMF is a prediction method based on the degree distribution, which can also be used for sparse Erdős-Rényi graphs. In our paper, we will show that also HMF suffers from overestimation because correlations are ignored.

An attempt to correct NIMFA and take correlations into account is done in [5] with a second order approximation. Drawbacks are that it leads to a system with  $n^2$  unknowns, and that its solutions might be unstable and physically meaningless. Other authors also propose methods to include higher-order effects. Usually these methods have improved accuracy at the cost of more computations. For instance Gleeson [15] proposes to solve a set of coupled differential equations, but also this is computationally challenging in larger networks. For a more complete overview, we refer to [26].

Our main contributions can be found in Section 2.4, after the definitions (Section 2.1) and a discussion on annealed and quenched prediction (Section 2.3). An important conclusion is that simple averaging arguments are insufficient to get accurate predictions, especially when degrees in the graph are small. It is then important to take the exact degree distribution and correlations between nodes into account. We will present ways to do this and heuristics to accurately predict the infected fraction and related quantities. These methods are suitable to be applied beyond Erdős-Rényi graphs.

## 2 Preliminaries and goals

### 2.1 Model definitions

The goal of this paper is to predict and understand the behaviour of the contact process on Erdős-Rényi graphs. In particular we are interested in the quasi-stationary behaviour. Which fraction of the population will be infected on average if the process has reached its metastable equilibrium?

We denote the set of nodes in our Erdős-Rényi graph by  $V = \{1, 2, \dots, n\}$ . Each pair of nodes  $\{i, j\}$  is connected (notation:  $i \sim j$ ) with probability  $p$ , independent of all other pairs. This random graph is denoted  $G_{n,p}$ . We typically take  $p$  to be a decreasing function of  $n$ . For instance, if  $p = c/n$  for some constant  $n$ , the average degree does not depend on the size of the population. In this case  $c$  has to be greater than 1, otherwise the graph only has small components which do not interact. If  $c > 1$ , there is a unique *giant* component, containing a positive fraction of the population also for  $n \rightarrow \infty$ . The graph then is called

supercritical. All Erdős-Rényi graphs in this paper are assumed to satisfy this criterion. Another threshold is  $p = \log(n)/n$ , when (almost) all nodes are in the giant.

On such an Erdős-Rényi graph  $G = (V, E)$ , we define our SIS process. This process is a continuous-time Markov process, with state space  $2^V$ . The state represents the set of infected nodes. Suppose  $I \subseteq V$  is the set of infected nodes. The transition rates are then defined by

$$\begin{aligned} I &\rightarrow I \setminus \{i\} \text{ with rate } \delta, \text{ for all } i \in I, & (\text{healing}) \\ I &\rightarrow I \cup \{j\} \text{ with rate } \#\{i \in I : i \sim j\} \cdot \tau, \text{ for all } j \in V \setminus I. & (\text{infection}) \end{aligned}$$

The healing rate for each infected node is  $\delta$ . Throughout this paper, we will stick to the convention that  $\delta = 1$ , without loss of generality. The infection rate of an infected node to each of its healthy neighbors is  $\tau$ . Also for  $\tau$ , we will often take a function of  $n$ .

For each node  $i$ , we let  $X_i(t)$  denote the status of node  $i$  at time  $t$ , where  $X_i(t)$  is either 1 (infected) or 0 (healthy). The total number of infected nodes at time  $t$  is denoted by  $X(t)$ . Furthermore, we let

$$\bar{X}(t) = \frac{1}{n} \sum_{i=1}^n X_i(t) = \frac{X(t)}{n}$$

denote the infected fraction of the population at time  $t$ . Quasi-stationarity means that the probability distribution of these quantities is (almost) independent of  $t$  in a large time window. Such behaviour will happen if the parameters admit a non-trivial state where healings and infections are balanced. For the complete graph, it is known that the quasi-stationary distribution is a well-defined object. This requires taking limits of  $n$  and  $t$  in the right way, see [1]. Similar behaviour is observed to appear in other graphs, in particular Erdős-Rényi graphs. Figure 1 clearly shows that the time evolution of the number of infected individuals fluctuates around some kind of equilibrium. In this paper we aim at predicting and understanding this equilibrium.

## 2.2 A naive prediction for the infected fraction

The quasi-stationary distribution of the number of infected individuals is known for the contact process on the complete graph. Suppose the process has healing rate 1 and infection rate  $\tau = \lambda n^{-1}$  (for some constant  $\lambda > 1$ ). The number of infected nodes then has a normal (quasi-)stationary distribution with expectation  $(1 - \lambda^{-1})n$  and variance  $\lambda^{-1}n$ , see [1]. This result can be used for a first naive prediction for the metastable infected fraction in an Erdős-Rényi graph.

Consider the contact process with infection rate  $\tau$  on the Erdős-Rényi graph  $G_{n,p}$ . An infected node can only infect a healthy node if there is an edge between them. Now assume that the event of two nodes being connected is independent of the event that exactly one of them is infected<sup>1</sup>. The product

<sup>1</sup>This assumption is reasonable if degrees are not too small. In reality we expect connected

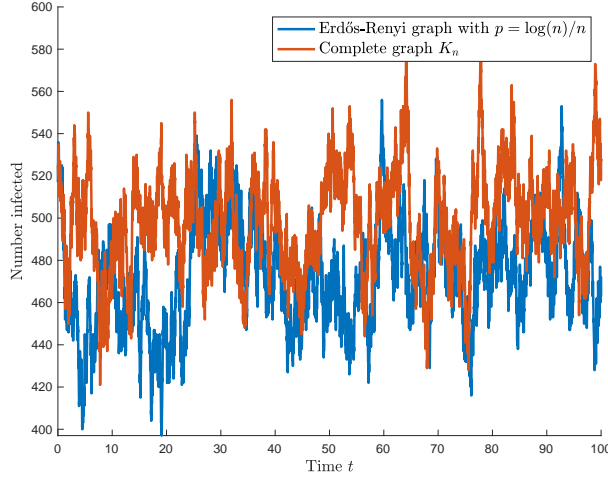


Figure 1: Number of infected nodes over time for the complete graph and an Erdős-Rényi graph. In both cases  $n = 1000$  and the effective infection rate  $p\tau$  is equal to  $2/n$ , see the discussion in Section 2.2

$p\tau$  could then be interpreted as the expected infection rate between a random infected and a random healthy node and will be called the *effective infection rate* of the process. Heuristically, the behaviour on an Erdős-Rényi graph with edge probability  $p$  and infection rate  $\tau$  should be comparable to the behaviour on the complete graph with the same effective infection rate. To guarantee that the infected fraction of the population stays away from 0 and 1, we take  $p\tau$  of order  $n^{-1}$  so that we can write  $p\tau = \lambda n^{-1}$  for some constant  $\lambda > 1$ . Based on the heuristic that the effective infection rate determines the quasi-stationary infected fraction, comparison with the complete graph (which is  $G_{n,p}$  with  $p = 1$ ) gives the following prediction

**Heuristic 1.** *Consider the contact process on an Erdős-Rényi graph  $G_{n,p}$  with effective infection rate  $p\tau = \lambda n^{-1}$ . The quasi-stationary distribution satisfies*

$$X \sim N(\mu, \sigma^2), \quad \text{with} \quad \mu = \left(1 - \frac{1}{\lambda}\right)n, \quad \sigma^2 = \frac{n}{\lambda}.$$

We could make this into a heuristic for the infected fraction, by dividing by  $n$ . This gives

$$\bar{X} \sim N\left(1 - \frac{1}{\lambda}, \frac{1}{n\lambda}\right),$$

so the infected fraction converges to  $1 - \frac{1}{\lambda}$  if  $n \rightarrow \infty$ . The comparison with the complete graph only makes sense if the random graph is (almost) connected, i.e.

---

nodes to be positively correlated, i.e. if they are connected, it is less likely that exactly one of them is infected. We will come back to this issue later.

the number of nodes outside the giant component should be negligible compared to  $n$ . This is equivalent to the number of isolated nodes being negligible [30]. For  $p = \log(n)/n$ , the expected number of isolated nodes is close to 1 for  $n \rightarrow \infty$ . So we should take  $p$  at least of this order. For practical reasons, in our simulations we will mostly restrict to the case  $\lambda = 2$ . We think that other choices give qualitatively similar behaviour.

To assess Heuristic 1, we did a simulation of the SIS process on the Erdős-Rényi graph with  $n = 1000$ ,  $p = \log(n)/n$  and  $\lambda = \tau np = 2$  for  $t \in [0, 100]$ . Heuristic 1 predicts that on average half of the population will be infected in the quasi-stationary situation. To get quick convergence to quasi-stationarity, we take each node to be infected with probability  $1/2$  independently at  $t = 0$ . We also did the simulation on the corresponding complete graph, so again with  $\lambda = 2$ . Figure 1 shows the time evolution of the two processes.

Taking the average over time, the process on the complete graph has half of the population infected (this has been rigorously proved in [1]). Apparently, the average infected fraction in *this realization* of the Erdős-Rényi graph is lower, the picture shows an average around 470. Since we look at random graphs, the average infected fraction depends on the graph and might be different if we generate a new Erdős-Rényi graph. It could still be that the heuristic works well if we would average over multiple realizations of the Erdős-Rényi graph. We therefore repeated the simulation and generated 10 independent realizations of the Erdős-Rényi graph (all with  $n = 1000$  and  $p = \log(n)/n$ ). On each of these graphs, we simulated the contact process with effective infection rate  $p\tau = 2/n$  for  $0 \leq t \leq 1000$ . See Figure 2 for the (approximated) quasi-stationary distribution for each of the graphs and a comparison with the quasi-stationary distribution of the complete graph.

Based on Figure 2, there seems to be a systematic error in Heuristic 1, which does not vanish if we would average over multiple realizations of the Erdős-Rényi graph. The mean of the quasi-stationary distribution is typically smaller than  $n/2$ . Apparently Heuristic 1 is too naive. One reason is that the infected set is not a uniform selection of nodes. This is an essential difference with the complete graph, where transition rates only depend on the size of the infected set, not on the exact selection of infected nodes. In Erdős-Rényi graphs, nodes with higher degrees are more likely to be in the infected set. Another point is that there are local effects: neighbors tend to be infected or healthy simultaneously. These differences make the model more realistic, but at the same time more complicated. We can not just take averages over all nodes as in the complete graph, but need more subtle prediction methods.

### 2.3 Annealed and quenched predictions

When looking at Figure 2, we see that the distribution in the Erdős-Rényi graph is not only clearly different from the complete graph, but also depends on the realization of the graph. For a given graph  $G$ , we can estimate the metastable distribution by simulating the SIS process on this particular graph. The corresponding random variable depends on  $G$  and on the infection rate

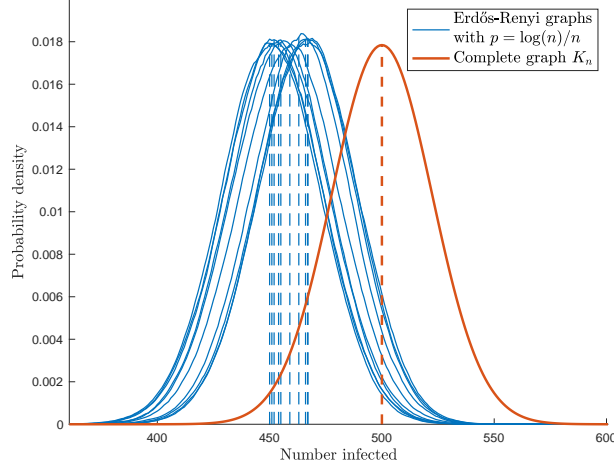


Figure 2: Probability distribution of the number of infected nodes in the complete graph (red) and in 10 realizations of the Erdős-Rényi-graph (blue), all with effective infection rate  $2/n$ . Dashed lines indicate means.

$\tau$  and is denoted  $X(G, \tau)$ . Given  $G$ , the metastable mean infected number is a constant  $\mu(G, \tau) := \mathbb{E}[X(G, \tau) \mid G]$ . The expectation is taken with respect to the randomness of the process, not of the graph. We will call  $\mu(G, \tau)$  the *quenched mean* and  $\mu(G, \tau)/n$  the *quenched infected fraction*. Each blue curve in Figure 2 has its own quenched mean. Similarly, we denote the quenched variance by  $\sigma^2(G, \tau)$ .

If we take the graph to be random, then  $\mathbb{E}[X(G, \tau)]$  becomes a random variable. Now we can take the expectation over the randomness of the graph as well to find the constant  $\mathbb{E}[\mathbb{E}[X(G, \tau)]]$ . This is what we will call the *annealed mean*. The annealed mean is independent of the graph realization and can be simulated by generating a bunch of graphs, running the process on each of them and taking the average of their metastable quenched means. For the SIS process on Erdős-Rényi graphs, the annealed mean is a function of the parameters which we denote by  $\mu(n, p, \tau)$ .

This gives rise to two different questions concerning prediction of the metastable infected fraction (or other quantities) in  $G = G_{n,p}$ :

1. **Annealed prediction:** given  $n$ ,  $p$  and  $\tau$ , predict  $\mu(G, \tau)$ , without observing  $G$ . The prediction will be a function  $\hat{\mu}(n, p, \tau)$ .
2. **Quenched prediction:** given the realization of  $G$ , predict  $\mu(G, \tau)$  using the graph information. The prediction will be a function  $\hat{\mu}(G, \tau)$ .

When doing quenched prediction, we are estimating the constant  $\mu(G, \tau)$ . The metastable infected fraction is some complicated function of  $G$  and  $\tau$  which in principle could be determined exactly. However, when doing an annealed

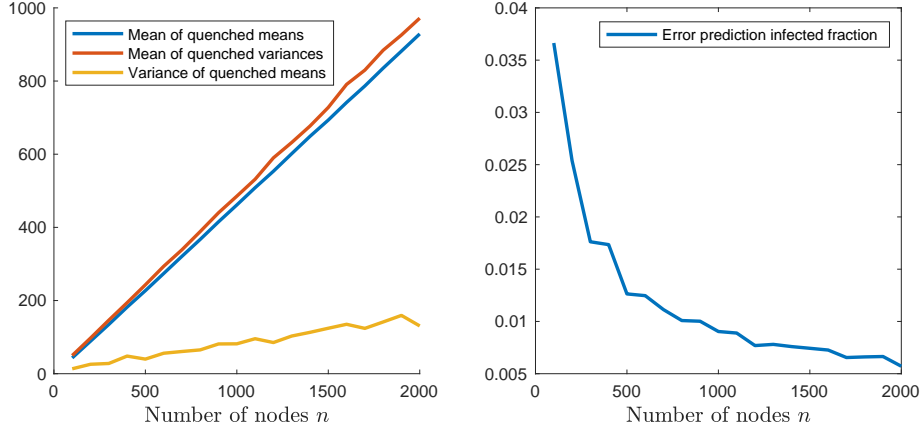


Figure 3: Left: Fixing an Erdős-Rényi graph, the metastable number of infected has mean (blue) and variance (red) both close to  $n/2$ . Varying the graph, the means themselves also fluctuate with a variance of order  $n$  (yellow). Right: Approximate minimal standard error for any annealed method to predict a quenched infected fraction.

prediction, the realization of  $G$  is not known and  $\mu(G, \tau)$  is a random variable. This means that we will always make errors caused by the variation of this random variable. It therefore makes sense to investigate the order of the variance of  $\mu(G, \tau)$  when  $G$  is random.

To do this, we generated for different values of  $n$ , realizations  $G_n^{(1)}, \dots, G_n^{(100)}$  of an Erdős-Rényi graph  $G_{n,p}$  with edge probability  $p = \log(n)/n$ . On each of them, we simulated the quenched mean  $\mu(G_n^{(k)}, \tau)$  and quenched variance  $\sigma^2(G_n^{(k)}, \tau)$  of the metastable distribution of the process with  $\lambda = 2$ . Then we took averages over  $k$  to obtain the mean of quenched means and the mean of quenched variances. Plotting them (Figure 3, left) shows that quenched means and quenched variances both grow linearly in  $n$ . In fact they are both close to  $n/2$ , as could be expected by comparing to the complete graph (cf. Heuristic 1).

Important is that also the variance of the quenched means appears to grow linearly with  $n$ . This means that annealed estimates for  $\mu(G, \tau)$  will always have errors of the same order as fluctuations in the metastable distribution (i.e. the square root of the quenched variance). Therefore, graph information is for all graph sizes of significant importance to make accurate predictions. Taking the square root of the variance of the quenched means and dividing by  $n$  gives the standard deviation in annealed prediction of  $\mu(G, \tau)$ , see right plot in Figure 3. For instance, for  $n = 1000$ , the standard deviation is about 0.01. This means that any annealed estimation method for the infected fraction will make errors of at least this order.



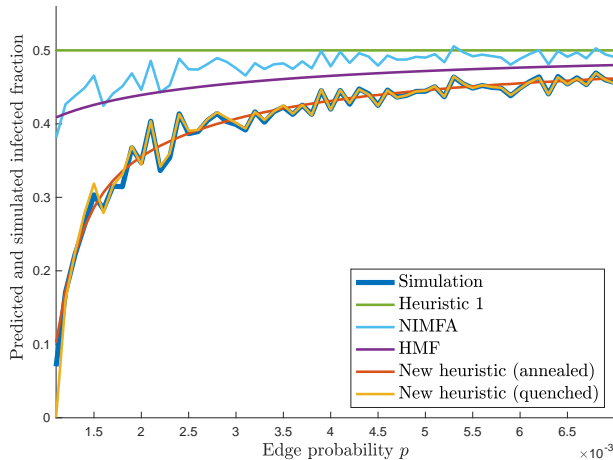


Figure 4: Simulated infected fraction compared to different predictions. Annealed methods are smooth, quenched methods follow the fluctuations of the simulation.

This point is once again illustrated in Figure 4. Here we see simulations of infected fractions in Erdős-Rényi graphs of size  $n = 1000$  for different values of  $p$ . Some of these predictions are annealed (corresponding to the smooth curves) and some of them are quenched (the non-smooth curves). The quenched predictions fluctuate much more, but follow the simulation result much better. An annealed prediction can never predict these fluctuations, because they are caused by the randomness of the graph.

Figure 4 also shows that HMF systematically overestimates the infected fraction in these sparse graphs. The same holds for NIMFA, although it clearly follows the random fluctuations of the simulation due to the quenched nature of NIMFA. Actually, HMF could also be interpreted as a quenched method, but this would not repair its bias. The new heuristics presented in this paper are much more accurate, both its annealed and quenched versions.

## 2.4 Main results

The main result of this paper is a new method to predict the infected fraction for connected graphs. It is designed for graphs which are locally tree-like and have degree distribution with exponential tails. This includes Erdős-Rényi graphs, random regular graphs and configuration model graphs with suitable degrees. The algorithm works as follows:

Algorithm to predict the metastable infected fraction in a connected graph  $G$  with  $n$  nodes. Infection rate:  $\tau$ . Healing rate: 1.

1. Let  $D$  be the degree distribution. Compute

$$P(d) := \mathbb{P}(D = d), \quad \tilde{P}(d) := d \cdot \mathbb{P}(D = d) / \mathbb{E}[D]. \quad (1)$$

2. For each pair of degrees  $(d_i, d_j)$ , define a matrix  $Q := Q(\eta, \tilde{\mu})$  by

$$Q = \begin{pmatrix} -\sum_{\ell \neq 1} Q_{1,\ell} & (d_j - 1)\eta\tilde{\mu}\tau/n & (d_i - 1)\eta\tilde{\mu}\tau/n & 0 \\ 1 & -\sum_{\ell \neq 2} Q_{2,\ell} & 0 & ((d_i - 1)\eta\tilde{\mu}\tau/n) + \tau \\ 1 & 0 & -\sum_{\ell \neq 3} Q_{3,\ell} & ((d_j - 1)\eta\tilde{\mu}\tau/n) + \tau \\ 0 & 1 & 1 & -\sum_{\ell \neq 4} Q_{4,\ell} \end{pmatrix}. \quad (2)$$

and determine the solution  $\mathbf{x}(d_i, d_j)$  (as function of  $\eta$  and  $\tilde{\mu}$ ) of

$$\begin{cases} \mathbf{x}^T Q = \mathbf{0}^T, \\ \mathbf{x}^T \mathbf{1} = 1, \end{cases} \quad \mathbf{x}^T = (x_1 \quad x_2 \quad x_3 \quad x_4), \quad (3)$$

where  $\mathbf{0}$  and  $\mathbf{1}$  are the all zero and all one vector in  $\mathbb{R}^4$ .

3. Determine  $\eta$  and  $\tilde{\mu}$  by solving the equations

$$\frac{\tilde{\mu}}{n} = \sum_{d_i} \sum_{d_j} P(d_i) \tilde{P}(d_j) (x_2(d_i, d_j) + x_4(d_i, d_j)) \quad (4)$$

$$\frac{\eta\tilde{\mu}}{n} = \sum_{d_i} \sum_{d_j} P(d_i) \tilde{P}(d_j) \frac{x_2(d_i, d_j)}{x_1(d_i, d_j) + x_2(d_i, d_j)}. \quad (5)$$

4. Estimate the infected fraction by

$$\frac{\mu}{n} = \sum_{d_i} \sum_{d_j} P(d_i) \tilde{P}(d_j) (x_3(d_i, d_j) + x_4(d_i, d_j)). \quad (6)$$

This algorithm extends HMF by incorporating correlations. It will be mathematically motivated and discussed in detail in Section 4. We did extensive simulations (Section 5), which show that in sparse graphs the algorithm is much more accurate than existing methods, including HMF and NIMFA. Our simulations test the algorithm for Erdős-Rényi graphs. These graphs are not necessarily connected, but the algorithm can still be used with small adaptations (see Heuristic 5 later in the paper). If a substantial fraction of the nodes is not in the giant component, best is to take this giant component as the graph to which the algorithm is applied. In that case, the degree distribution will depend on the edge density, so that the algorithm is automatically tested for different

degree distributions.

We will also discuss quenched variants of our heuristic, which typically give more accurate results, but might complicate the computations. The most advanced quenched version would use the full graph structure and would be an extension of NIMFA. It seems however that the same quality of prediction can already be reached by simpler variants, using only the degree sequence or even only the sum of the degrees.

Our heuristic also gives the tools to estimate quantities other than the infected fraction, like fluctuations around the metastable equilibrium and correlations between neighboring nodes.

The algorithm is computationally very friendly. One has to solve a number of small linear systems in step 2 of the algorithm, and then  $\eta$  and  $\tilde{\mu}$  can be determined iteratively. For instance, for an Erdős-Rényi graph with  $n = 10^7$ ,  $p = \log(n)/n$  and  $\lambda = 2$ , the calculation needs only a fraction of a second. The reason is that the computation time grows like the maximal degree squared, i.e. like  $\log(n)^2$ . For comparison: NIMFA would require to solve a non-linear system of  $n$  equations in  $n$  unknowns, which would hardly be feasible. Other methods as in [5, 15] which do try to incorporate correlations are even much worse from a computational point of view.

Finally, an important point to take away is that it gets more and more delicate to make accurate predictions when graphs get sparser. Sparseness makes averages less reliable, correlations more important and heuristics more sensitive to errors.

### 3 Improved heuristics for the infected fraction

In this section we start to gradually build towards our main prediction method which will be presented in Section 4.

When predicting the metastable infected fraction in an Erdős-Rényi graph, the graph structure and in particular the degree distribution is of key importance. In this section we show how to use the degrees to design more accurate prediction methods. One of these methods will turn out to be equivalent to NIMFA, another to HMF.

The methods in this section, although much better than Heuristic 1, still have their shortcomings. We will explain where it goes wrong, and in particular why NIMFA and HMF have a serious bias in sparse graphs. Nevertheless, the ideas in this section are the basis for the exposition of more sophisticated methods in Section 4.

#### 3.1 Nodes with higher degree are more frequently infected

Both in the Erdős-Rényi graph and in the complete graph, the fraction of nodes that is infected is close to  $1 - \lambda^{-1}$  and is quite stable over time, see again Figure 1. This also means that on average nodes are infected about a fraction  $1 - \lambda^{-1}$  of time.

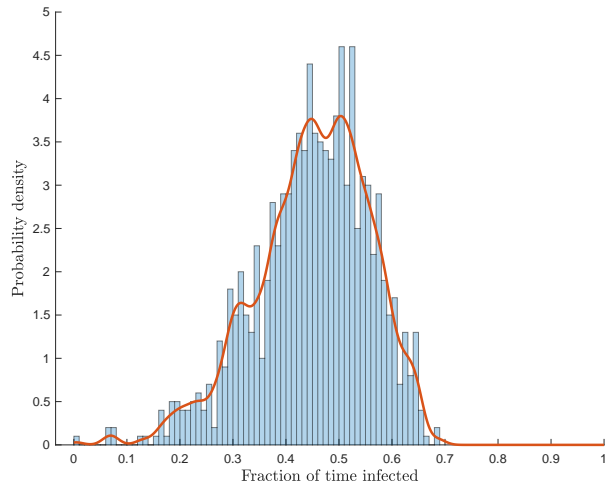


Figure 5: Simulated and estimated probability density of the fraction of time a node is infected.

Since nodes are indistinguishable in the complete graph, each individual node is expected to be infected the same fraction of time. In the complete graph ( $n = 1000, \lambda = 2$ ), *all* nodes are infected about half of the time. If we send the running time (not too fast, to avoid extinction) and the number of nodes to infinity, this fraction of time will converge to  $1/2$  for each individual node. To illustrate, we ran the process on the complete graph for  $10^5$  units of time and found that 99% of the nodes was infected between 49.5 and 50.3% of the time.

The fraction of time an individual node is infected could be quite different in the Erdős-Rényi graph. In Figure 5, we see a histogram of these fractions of time and an estimate of the density function (using kernel density estimation). In this Erdős-Rényi graph ( $n = 1000, p = \log(n)/n, \lambda = 2$ ), nodes are only *on average* infected about half of the time. The fraction of time an individual node is infected ranges from 0 to about 0.7. For each individual node it will converge if the running time of the process increases, but the limiting fraction for each node will depend on the geometry of the graph.

The degree of a node can be used to give quite a good prediction for the fraction of time this node will be infected. This in turn will explain the shape of the density function in Figure 5. In first approximation, the fraction of time a randomly picked node is infected is equal to  $1 - \lambda^{-1}$ . It therefore infects each of its neighbors at rate

$$\tau - \frac{\tau}{\lambda}.$$

Let  $i$  be a random node with degree  $d = d_i$ . The fraction of time this node is infected will be called  $f_i$ . Assume that its neighbors are ‘random’ nodes. Then

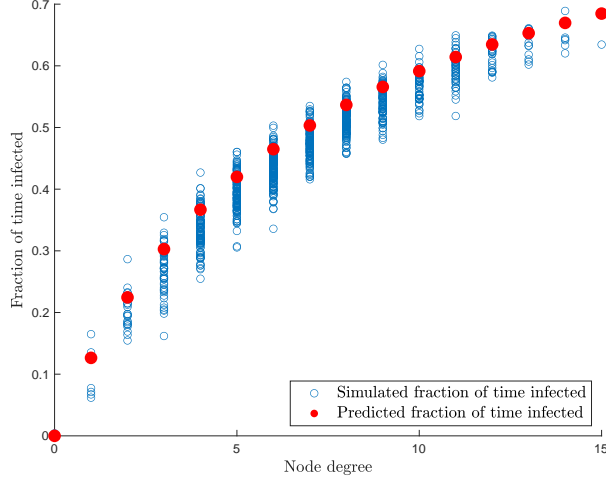


Figure 6: Simulation of the fraction of time nodes are infected, plotted as points  $(d_i, f_i)$  in blue. The red markers indicate the degree-dependent prediction  $(d, f(d))$  based on the heuristic (7).

$i$  is healing at rate 1 and, since it has  $d$  neighbors, getting infected at rate

$$d\tau - \frac{d\tau}{\lambda}.$$

If we consider a Markov process with one node, which is healing at rate 1 and getting infected at rate  $\alpha$ , in the stationary distribution this node is infected a fraction  $\alpha/(1 + \alpha)$  of time. Therefore, in our more complicated model, the fraction of time  $i$  is infected can be estimated by

$$\hat{f}_i := \frac{d\tau - \frac{d\tau}{\lambda}}{1 + d\tau - \frac{d\tau}{\lambda}}. \quad (7)$$

Fixing the parameters of the graph and the process, this estimate only depends on  $d$ , so we write  $f(d)$  for  $\hat{f}_i$ . In Figure 6, we plotted the points  $(d, f(d))$  and compare with all the points  $(d_i, f_i)$  obtained by simulation of the contact process on an Erdős-Rényi graph ( $n = 1000, p = \log(n)/n, \lambda = 2$ ).

In Figure 7, we compare the empirical distribution function of the per-node infected fraction of time,

$$\frac{1}{n} \sum_{i=1}^n \mathbb{1}\{f_i \leq x\},$$

with the quenched estimated cumulative distribution function

$$\frac{1}{n} \sum_{i=1}^n \mathbb{1}\{f(d(i)) \leq x\}.$$

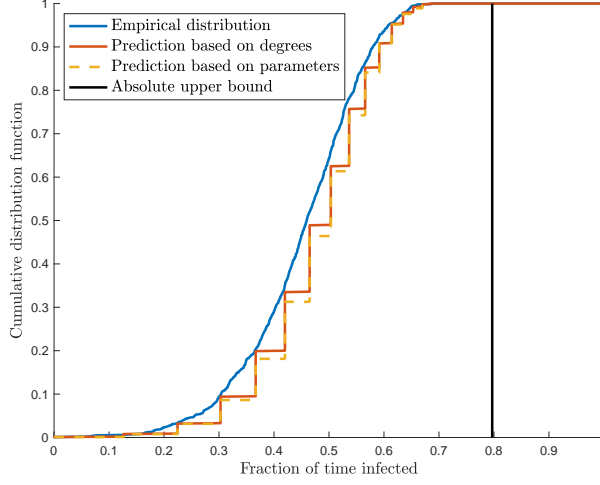


Figure 7: Cumulative distribution of infected fraction of time. Blue: empirical. Red: quenched prediction. Green: annealed prediction. Both predictions have jumps at the values  $f(d)$ . Black: absolute upper bound for the infected fraction caused by the maximal degree.

To compute this estimation, we need the actual degrees in the graph. Since we know that the degree distribution  $D$  in the graph is  $\text{Bin}(n-1, p)$ , we can also estimate the distribution without observing the actual degrees by

$$\frac{1}{n} \sum_{i=1}^n \mathbb{1}\{f(d(i)) \leq x\} = \sum_{d=0}^{n-1} \frac{\#\{i : d_i = d\}}{n} \cdot \mathbb{1}\{f(d) \leq x\} \quad (8)$$

$$\approx \sum_{d=0}^{n-1} \mathbb{P}(D = d) \cdot \mathbb{1}\{f(d) \leq x\} \quad (9)$$

$$= \sum_{d=0}^{n-1} \binom{n-1}{d} p^d (1-p)^{n-1-d} \cdot \mathbb{1}\{f(d) \leq x\}. \quad (10)$$

This prediction as well is compared with the observed empirical distribution in Figure 7. Note that this is an annealed prediction: it can be computed using only the three parameters  $n$ ,  $p$  and  $\tau$ .

If the maximal degree  $\Delta$  in the graph is known, we can compute an absolute upper bound for the (limiting) fraction of time a node is infected. Let  $\theta$  be the maximal fraction of time a node is infected. Let  $i$  be a node in the graph. If all its neighbors are infected all the time, then  $i$  is infected at rate at most  $\Delta\tau$ . It follows that

$$\theta \leq \frac{\Delta\tau}{1 + \Delta\tau} < 1. \quad (11)$$

A sharper heuristic upper bound is obtained by the using positive correlations between  $i$  and its neighbors (shown in [9, 7]). The neighbors of  $i$  also are infected at most a fraction  $\theta$  of time. Positive correlations mean that this upper bound still holds when restricting to periods when  $i$  is healthy. Therefore,  $i$  is infected at rate at most  $\Delta\tau\theta$ . This implies that

$$\theta \leq \frac{\Delta\tau\theta}{1 + \Delta\tau\theta}. \quad (12)$$

It follows that  $\theta$  is at most equal to the largest solution of (12), which is given by

$$\frac{\tau\Delta - 1}{\tau\Delta}.$$

In our example in Figure 7, we have  $\tau = 2/(np) = 2/\log(1000) \approx 0.29$  and  $\Delta = 17$ . This gives approximately 0.79 as an absolute upper bound for the fraction of time a node can be infected, see the vertical line in the plot.

Note that  $\Delta = n - 1$  in the complete graph  $K_n$ , giving the upper bound  $1 - 1/((n - 1)\tau) \approx 1 - 1/\lambda$ . This is consistent with known results for  $K_n$ , see [1].

### 3.2 Degree-based heuristics for the infected fraction

The idea of estimate (7) will be used to predict the infected fraction  $\mu/n = \mathbb{E}\bar{X}$  of the population. In the previous section, we estimated  $\mu/n$  by  $1 - \lambda^{-1}$ , based on Heuristic 1. We will derive a heuristic equation for  $\mu/n$ , leading to an improved estimate. Let  $i$  be a node with degree  $d$  and assume that its neighbors are infected a fraction  $\mu/n$  of time. Analogous to (7), we estimate the fraction of time  $i$  is infected by

$$\hat{f}_i := \frac{d\tau\mu/n}{1 + d\tau\mu/n}. \quad (13)$$

A very similar formula is derived in [27], as the stationary solution of the differential equation

$$\partial_t f(d, t) = -f(d, t) + \tau d(1 - f(d, t))\Theta(t). \quad (14)$$

Here  $f(d, t)$  is the probability a node of degree  $d$  is infected at time  $t$ , and  $\Theta(t)$  is the fraction of half-edges connected to an infected node. Note that  $\Theta(t)$  is not exactly the same as the infected fraction of the population at time  $t$ . We will come back to this in Section 3.3. In stationarity,  $\Theta(t)$  does not depend on  $t$ , and setting the derivative in (14) equal to zero gives the analogue of (13).

Averaging the quantity  $\hat{f}_i$  over all nodes in the graph, we obtain an estimate for  $\mu/n$ . Hence, if  $n$ ,  $p$  and  $\tau$  are given,  $\mu/n$  can be predicted by (numerically)

solving

$$\frac{\mu}{n} = \frac{1}{n} \sum_{i=1}^n \hat{f}_i \quad (15)$$

$$= \sum_{d=0}^{n-1} \frac{\#\{i : d_i = d\}}{n} \cdot \frac{d\tau\mu/n}{1 + d\tau\mu/n} \quad (16)$$

$$\approx \sum_{d=0}^{n-1} \binom{n-1}{d} p^d (1-p)^{n-1-d} \cdot \frac{d\tau\mu}{n + d\tau\mu}. \quad (17)$$

In fact the right hand side is the expectation  $\mathbb{E}[\tau\mu D/(n + \tau\mu D)]$ . Therefore, by Jensen's inequality, (17) implies

$$\frac{\mu}{n} \leq \frac{\tau\mu\mathbb{E}[D]}{n + \tau\mu\mathbb{E}[D]}. \quad (18)$$

Solving for  $\mu/n$  gives  $\mu/n \leq 1 - 1/\lambda$ , so that this procedure to predict the infected fraction always gives a lower estimate than Heuristic 1.

For large  $n$  and  $d$ , the binomial probabilities in (17) are hard to compute, but they are well approximated by using the central limit theorem,

$$\mathbb{P}(\text{Bin}(n-1, p) = d) \approx \mathbb{P}(|N((n-1)p, (n-1)p(1-p)) - d| \leq \tfrac{1}{2}) \quad (19)$$

$$= \Phi\left(\frac{d - (n-1)p + \frac{1}{2}}{\sqrt{(n-1)p(1-p)}}\right) - \Phi\left(\frac{d - (n-1)p - \frac{1}{2}}{\sqrt{(n-1)p(1-p)}}\right), \quad (20)$$

where  $\Phi$  is the cumulative distribution function of the standard normal. This gives us

**Heuristic 2.** Consider the contact process on an Erdős-Rényi graph  $G = G_{n,p}$  with infection rate  $\tau$ . The quasi-stationary infected fraction  $\mu/n$  satisfies

$$\frac{\mu}{n} = \sum_{d=0}^{n-1} P(n, p, d) \cdot \frac{d\tau\mu}{n + d\tau\mu}. \quad (21)$$

Here  $P(n, p, d)$  is either

- (a) The probability  $\mathbb{P}(\text{Bin}(n-1, p) = d)$  or an approximation to it.
- (b) The exact frequency  $\#\{i : d_i = d\}/n$ .

Note that (a) gives an annealed prediction, while (b) is a quenched prediction. In view of earlier discussions, we expect (b) to be more accurate.

For  $n \rightarrow \infty$ , the probability mass of the degree distribution concentrates around its expectation  $np$  with standard deviation  $\sqrt{np(1-p)}$ . This means that for  $np \rightarrow \infty$  and  $\tau np = \lambda$  the right hand side of (21) converges to

$$\lim_{n \rightarrow \infty} \frac{np\tau\mu}{n + np\tau\mu} = \frac{\lambda \lim_{n \rightarrow \infty} \mu/n}{1 + \lambda \lim_{n \rightarrow \infty} \mu/n}.$$



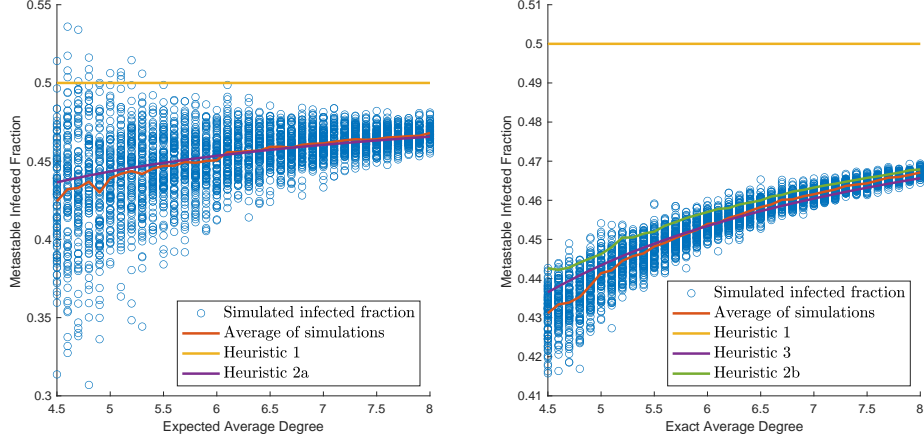


Figure 8: Infected fractions in Erdős-Rényi graphs with  $p = \log(n)/n$  and  $\tau = 2/\log(n)$ . Left: annealed prediction. Right: quenched predictions (the horizontal coordinate of each point depends on the graph.)

Solving (21) for  $\lim_{n \rightarrow \infty} \mu/n$ , we obtain

$$\lim_{n \rightarrow \infty} \frac{\mu}{n} = 1 - \frac{1}{\lambda}, \quad (22)$$

so that both versions of Heuristic 2 coincide with Heuristic 1 for  $n \rightarrow \infty$ . The advantage of taking  $P(n, p, d)$  as a probability (as in Heuristic 2a) is that we do not need to know degrees in the graph.

### 3.2.1 Simulation and annealed prediction for $p = \log(n)/n$

We test Heuristic 2a, taking edge probability  $p = \log(n)/n$  and using the normal approximation (20). The average degree in the graph is then about  $\log(n)$ , which is just enough to get an (almost) connected graph. For each  $n = \lceil e^{k/10} \rceil$ ,  $k = 45, 46, \dots, 80$ , we generate 100 replications of the Erdős-Rényi graph so that in total we have 3600 graphs. The average degrees vary from 4.5 to 8 and the sizes range from 91 to 2981 nodes. On each of those graphs, we simulate the contact process with infection rate  $\tau = 2/\log(n)$ . With these choices, the effective infection rate is  $\lambda = 2$ , so the crude Heuristic 1 predicts that on average half of the population is infected.

Our simulation results are given in Figure 8, left plot. Each simulated graph is represented by a small blue circle. The horizontal coordinate is the expected average degree  $\log n$ . The vertical coordinate is the simulated infected fraction  $\bar{X}$ , averaged over time. This is an estimate for the quasi-stationary mean. The variance is decreasing, since the graph sizes are increasing from left to right. Note that the quasi-stationary mean depends on the realization of the graph, but the two heuristics do not: predictions are annealed.

### 3.2.2 Using graph information: quenched predictions

Heuristic 2a seems to do quite well on average in Figure 8, but there is a lot of variation in the simulation results. The prediction by Heuristic 2a can be computed by just using the parameters  $n$ ,  $p$  and  $\tau$ , so the prediction is annealed and can be made *before* generating the graph. Can we predict the stationary infected fraction more accurately *after* generating the graph and using characteristics of the graph? This would be quenched prediction.

To test this, we again generated Erdős-Rényi graphs with the same numbers of nodes as in Figure 8. If  $p = \log(n)/n$ , the expected total number of edges is  $p\binom{n}{2} = \frac{1}{2}(n-1)\log(n)$ . This time we conditioned the graphs to have the number of edges exactly equal to its (rounded) expectation. We can even eliminate the rounding error by slightly adjusting  $p$ . The simulation results are shown in Figure 8, right plot. The horizontal coordinate now is the *exact* average degree, since we fixed the number of edges to its expectation. For unconditioned ER-graphs, this exact average degree is a quenched parameter, which can only be computed after observing the graph.

It turns out that graphs with the same exact average degree have a lot less variation in their quasi-stationary means than graphs merely having the same expected average degree. So a lot of the variation is explained by variation of the number of edges in the graph. The prediction therefore becomes more accurate by the following quenched prediction method: first estimate  $p$  based on the observed number of edges, then use this adjusted  $p$  for estimating the metastable infected fraction. The resulting heuristic is:

**Heuristic 3.** *Let  $G$  be an Erdős-Rényi graph with  $n$  nodes and  $m$  edges. Consider the contact process on  $G$  with infection rate  $\tau$ . The quasi-stationary infected fraction  $\mu/n$  satisfies*

$$\frac{\mu}{n} = \sum_{d=0}^{n-1} P\left(n, \frac{m}{\binom{n}{2}}, d\right) \cdot \frac{d\tau\mu}{n + d\tau\mu}. \quad (23)$$

Here  $P(n, p, d)$  is an approximation to the probability  $\mathbb{P}(\text{Bin}(n-1, p) = d)$ .

The formula is the same as Heuristic 2a, but the point where we evaluate it depends on the graph. This prediction still seems to have a small systematic bias for some values of  $n$ . We will discuss systematic errors in Heuristic 2 and 3 in the next section.

Heuristic 3 uses the exact number of edges in the graph, which is equivalent to using the sum of the degrees. Next steps would be to use all individual degrees or even the full adjacency matrix  $A$  of the graph. If the full degree sequence is known, we could use Heuristic 2b with the exact numbers  $\#\{i : d_i = d\}$ . It turns out by simulations that this is more accurate than Heuristic 2a, but has a larger bias than Heuristic 3 in the simulated range, see again Figure 8. A remark to be made here is that now graphs with the same exact average degree might get different predictions. The curve for Heuristic 2b only shows the average of these

predictions. This means that prediction errors for individual graph realizations can not be seen in the picture.

To see individual errors, we simulated the contact process on 100 Erdős-Rényi graphs with  $n = 1000$  nodes,  $p = \log(n)/n$  and  $\lambda = 2$ . Figure 9 gives boxplots for the errors: the difference between the predicted infected fraction and the simulated infected fraction for the different heuristics. In particular this picture shows that quenched predictions are more accurate. Indeed, the errors for Heuristics 1 and 2a have much more variation. On the other hand, more detailed information than the number of edges does not really improve the predictions: Heuristic 3 is not worse than Heuristic 2b and 4 (these heuristics respectively use the exact number of edges, the exact degrees and the full adjacency matrix). Heuristic 4 (to be discussed next) has a small variation, but a large systematic error. The systematic errors of Heuristics 3 and 2b are relatively small, but the situation gets worse when the graph is more sparse, in particular when the graph disconnects. In that case one has to be more careful, see Section 5. In general, these heuristics work quite well on graphs which are fairly homogeneous such as the complete graph or Erdős-Rényi graph with enough edges. For less homogeneous graphs like power-law graphs, other heuristics are needed.

Now assume the full adjacency matrix is known. Writing again  $f_i$  for the fraction of time  $i$  is infected, and assuming independence between nodes, we find that  $i$  gets infected at rate  $\tau \sum_{j:i \sim j} f_j$ . Therefore  $f_i$  satisfies

$$f_i = \frac{\tau \sum_{j:i \sim j} f_j}{1 + \tau \sum_{j:i \sim j} f_j}. \quad (24)$$

It turns out that this is equivalent to NIMFA, which is derived as follows. Consider  $\mathbb{P}(X_i(t) = 1) = \mathbb{E}[X_i(t)]$ . By standard Markov chain theory, its derivative is expressed in the transition rates by

$$\frac{d}{dt} \mathbb{E}[X_i(t)] = -\mathbb{E}[X_i(t)] + \tau \sum_{j:i \sim j} \mathbb{E}[(1 - X_i(t)) \cdot X_j(t)], \quad (25)$$

where the first term on the right corresponds to healing of  $i$  and the second to infection. The NIMFA assumption is to ignore correlations by setting

$$\mathbb{E}[X_i(t) \cdot X_j(t)] = \mathbb{E}[X_i(t)] \cdot \mathbb{E}[X_j(t)]. \quad (26)$$

The stationary solution is then obtained by solving

$$0 = -\mathbb{E}[X_i] + \tau \sum_{j:i \sim j} \mathbb{E}[X_j] + \tau \mathbb{E}[X_i] \sum_{j:i \sim j} \mathbb{E}[X_j], \quad (27)$$

which is the same as (24). Solving this system of  $n$  non-linear equations and  $n$  unknowns gives a quenched prediction  $\hat{f}_i$ , after which the infected fraction of the population can be predicted by

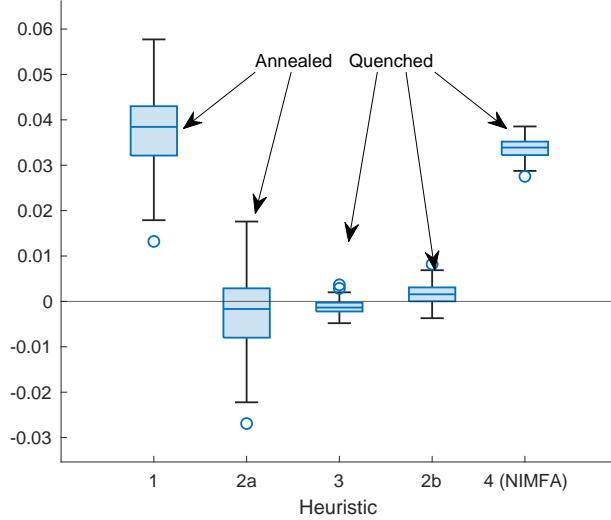


Figure 9: Error boxplots for each heuristic for Erdős-Rényi graphs with  $n = 1000$ ,  $p = \log(n)/n$  and  $\lambda = 2$ . The errors of annealed methods have a standard deviation of about 0.01, cf. Figure 3. The errors of quenched heuristics have smaller variation. Heuristic 1 and NIMFA are clearly biased.

**Heuristic 4 (NIMFA).** Let  $G = (V, E)$  be an Erdős-Rényi graph. Consider the contact process on  $G$  with infection rate  $\tau$ . Let  $\hat{f}_i, i \in V$  be the solution of the system (24). The quasi-stationary infected fraction  $\mu/n$  satisfies

$$\frac{\mu}{n} = \frac{1}{n} \sum_{i=1}^n \hat{f}_i. \quad (28)$$

One would expect this to be more accurate than Heuristic 2b. However, our simulations show NIMFA to be strikingly more biased for  $n = 1000$  and  $p = \log(n)/n$  (see Figure 9). This is a general problem with NIMFA in graphs with small degrees. In the next sections we explain how this is possible.

### 3.3 Systematic errors I: size bias and the infection paradox

Heuristics 2a, 2b and 3 are all based on the assumption that the neighbors of a random node  $i$  are infected a fraction  $\mu/n$  of time. However, given the information that  $j$  is a neighbor of  $i$ , the degree distribution of  $j$  is different. This is the so-called friendship paradox, and the degree distribution of  $j$  is called the size-biased distribution [30]. Precisely, the probability that  $j$  has degree  $d$  has to be weighted by a factor  $d$ . When all nodes independently have the same

degree distribution  $D$ , the degree  $D_j$  of  $j$  satisfies

$$\mathbb{P}(D_j = d \mid i \sim j) = \frac{d \cdot \mathbb{P}(D = d)}{\sum_d d \cdot \mathbb{P}(D = d)} = \frac{d \cdot \mathbb{P}(D = d)}{\mathbb{E}[D]}. \quad (29)$$

For the Erdős-Rényi graph, an exact expression is

$$\mathbb{P}(D_j = d \mid i \sim j) = \mathbb{P}(\text{Bin}(n-2, p) = d-1) = \binom{n-2}{d-1} p^{d-1} (1-p)^{n-d-1}. \quad (30)$$

For large  $n$  and small  $p$  and  $d$ , this results in

$$\mathbb{P}(D_j = d \mid i \sim j) \approx \frac{(np)^{d-1} (1-p)^n}{(d-1)!} \approx \frac{d \cdot \mathbb{P}(D_i = d)}{np}, \quad (31)$$

which is consistent with the general formula (29). Note that the formula in the middle is also approximately  $\mathbb{P}(D_i = d-1)$ , so that the degree distribution of  $j$  is obtained by shifting the original degree distribution by 1. Hence, in Heuristics 2a, 2b and 3 we make an error of 1 in counting the neighbors of  $j$ . This error causes an underestimation of the fraction of time neighbors of  $i$  are infected, which in turn also leads to underestimation for  $i$  itself.

The friendship paradox thus implies an infection paradox:

**Paradox 1.** *An average neighbor of an average node is more often infected than the node itself.*

In Figure 10 we see an illustration of this paradox. We simulated an Erdős-Rényi graph with  $n = 1000$ ,  $p = \log(n)/n$  and  $\tau = 2/\log(n)$ . For each node, we computed the fraction of time it was infected (horizontal axis) and the mean fraction of time its neighbors were infected (vertical axis). On average, nodes are infected 46.1% of time, but neighbors are infected 49.7% of time (black cross). Most of the points (606 out of 1000) are above the diagonal, meaning that neighbors of a node are more often infected than the node itself. Also the shape of the distribution is different: taking the average over neighbors gives a more concentrated distribution than directly looking at infection times of nodes.

Let again  $i$  be a random node and  $j$  a random neighbor of  $i$ . Instead of assuming that  $i$  and  $j$  themselves have the same degree distribution, now assume that neighbors of  $j$  have the same degree distribution as neighbors of  $i$ . Note that this assumption is still not entirely correct, we now essentially make an error of 1 in counting neighbors at distance 2 of  $j$ . In a tree-like graph this error is of a smaller order. Under this improved assumption, we obtain

$$\frac{\tilde{\mu}}{n} = \sum_{d=1}^{n-1} \mathbb{P}(\text{Bin}(n-2, p) = d-1) \cdot \frac{d\tau\tilde{\mu}}{n + d\tau\tilde{\mu}} \quad (32)$$

where  $\tilde{\mu}/n$  is the fraction of time a random neighbor of a random node is infected. This motivates to adapt Heuristic 2 and to estimate  $\mu/n$  by

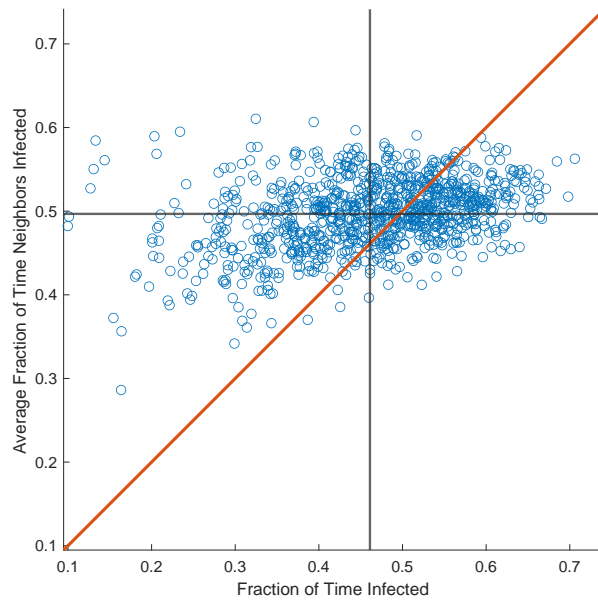


Figure 10: The infection paradox: most nodes are less often infected than their neighbors. Averages are indicated by the horizontal and vertical line, they intersect clearly above the diagonal.

**Heuristic 2** (Variant HMF). *Solve (32) for  $\tilde{\mu}$ . Then  $\mu$  satisfies*

$$\frac{\mu}{n} = \sum_{d=0}^{n-1} \mathbb{P}(\text{Bin}(n-1, p) = d) \cdot \frac{d\tau\tilde{\mu}}{n + d\tau\tilde{\mu}}. \quad (33)$$

In fact,  $\tilde{\mu}/n$  is the same as the stationary solution for  $\Theta$  appearing in (14). Moreover, though the derivation is slightly different, our formula (33) is exactly the same as the Heterogenous Mean Field method designed by Pastor-Satorras and Vespignani in [27].

The infection paradox leads to underestimation of  $\mu/n$ , so the adaptation in (33) will increase our previous estimates (Heuristics 2a, 2b and 3) for the infected fraction.

### 3.3.1 Mean-field methods NIMFA and HMF and size-bias

NIMFA uses the full adjacency matrix, which means that degrees of neighbors are always counted correctly. NIMFA therefore does not make a systematic error caused by size-bias. The same is true for HMF, which explicitly takes the size-bias effect into account. This explains why both these methods give higher estimates for the infected fraction than for instance Heuristic 2a. This can be clearly seen in Figure 11. We simulated ER-graphs with 1000 nodes and edge probability  $p$  between  $2 \cdot 10^{-3}$  and  $15 \cdot 10^{-3}$ , so the expected degrees vary from 2 to 15. For each  $p$ , 100 graphs were generated, and on each of them we simulated the contact process. Also for each graph, we calculated the predictions by NIMFA, HMF, and by the simpler Heuristics 1 and 2a. Again we see that Heuristic 1 is too simple, but 2a is much more accurate than HMF and NIMFA. Only when the graphs become really sparse with average degrees less than 5, Heuristic 2a visibly deviates from the simulation results. We will come back to this in Section 5.

By correcting for size-bias, NIMFA and HMF actually become *more* biased than other methods. The reason is that there are two sources of systematic errors, which work in opposite directions and which often seem to almost cancel each other. The second error source is caused by correlations, and will be discussed in the next section. By repairing only one of these errors, NIMFA and HMF get their bias, which especially will be visible in sparse graphs.

## 3.4 Systematic errors II: neighbor correlation

Another aspect we ignored so far is dependence between neighboring nodes. For NIMFA, this is an explicit assumption. Also the other heuristics discussed before do not take dependence into account. Neighbors tend to align into the same state. When a node  $i$  is healthy, this increases the likelihood of its neighbors being healthy as well, see [9, 7]. By ignoring this, we overestimate the rate at which  $i$  gets infected by its neighbors. For this reason, the paper introducing NIMFA [31] already mentions that the method gives an upper bound for the infected fraction.

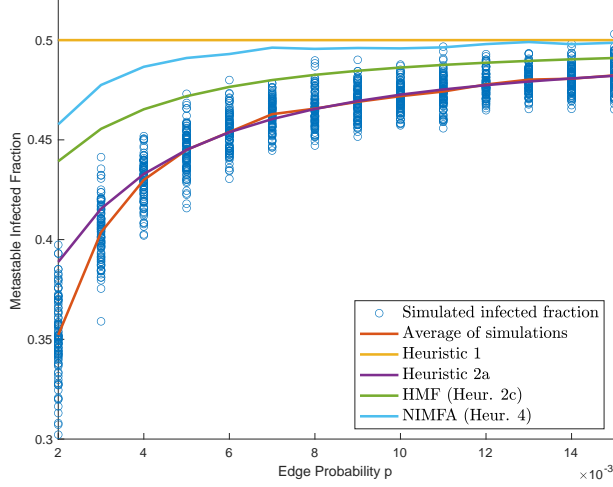


Figure 11: NIMFA and HMF systematically overestimate the infected fraction and are outperformed by Heuristic 2a.

To illustrate the phenomenon of neighbor correlation, we simulated the process on an Erdős-Rényi graph with  $n = 1000$  nodes,  $p = \log(n)/n$  and  $\lambda = 2$ . For each edge  $(i, j)$  in the graph, (co)variances are given by

$$\text{Var}(X_i) = \mathbb{E}(X_i^2) - (\mathbb{E}(X_i))^2 = \mathbb{P}(X_i = 1) - \mathbb{P}(X_i = 1)^2, \quad (34)$$

$$\begin{aligned} \text{Cov}(X_i, X_j) &= \mathbb{E}(X_i X_j) - \mathbb{E}X_i \cdot \mathbb{E}X_j \\ &= \mathbb{P}(X_i = X_j = 1) - \mathbb{P}(X_i = 1) \cdot \mathbb{P}(X_j = 1). \end{aligned} \quad (35)$$

These are estimated by the corresponding simulated fractions of time, after which we can also estimate the correlation coefficients

$$\rho(X_i, X_j) = \frac{\text{Cov}(X_i, X_j)}{\sqrt{\text{Var}(X_i)\text{Var}(X_j)}}. \quad (36)$$

In Figure 12, we plot the estimated correlation coefficients against the estimated product  $\mathbb{P}(X_i = 1) \cdot \mathbb{P}(X_j = 1)$ . As expected, the correlations are clearly positive. Further note that the correlation is weaker if the nodes are more often infected. This can be explained as follows: a node which is frequently infected has more neighbors, so that the influence of an individual neighbor is less important. In fact, taking on the horizontal axis the product of the degrees instead would give a similar picture.

All heuristics in the previous section use the assumption that the rate at which node  $i$  is infected by node  $j$  is equal to  $\tau \cdot \mathbb{P}(X_j = 1)$ . However, node  $j$  is only able to successfully infect  $i$  if  $i$  is healthy. Therefore, the actual rate at which  $j$  infects  $i$  is equal to

$$\tau \cdot \mathbb{P}(X_j = 1 \mid X_i = 0), \quad (37)$$



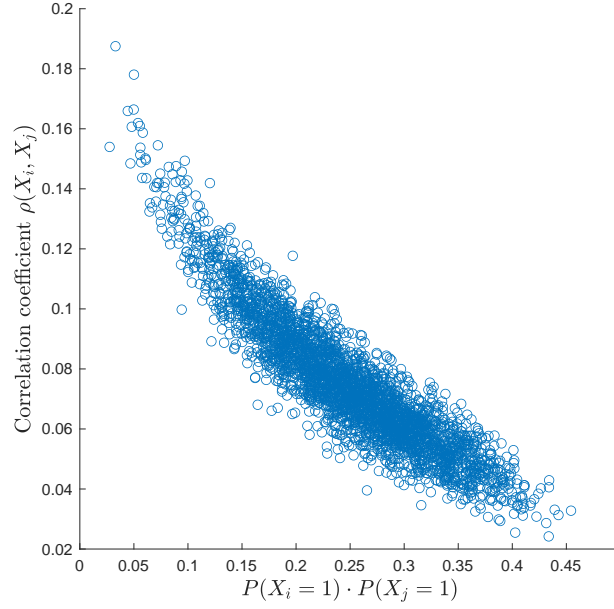


Figure 12: Neighbor correlations in Erdős-Rényi graph. Each marker represents an edge  $(i, j)$ .

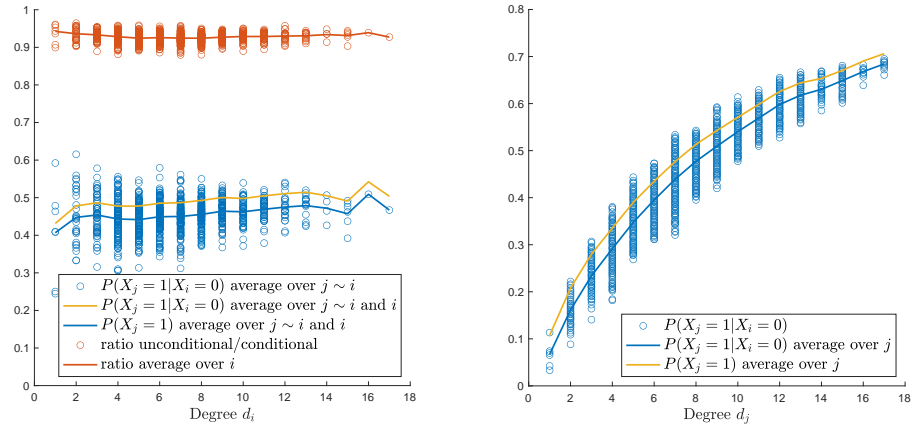


Figure 13: Dependence of conditional probabilities  $\mathbb{P}(X_j = 1 \mid X_i = 0)$  on the degrees  $d_i$  and  $d_j$ .

which is smaller than  $\tau \cdot \mathbb{P}(X_j = 1)$  due to correlations. In Figure 13, we see how the conditional probability  $\mathbb{P}(X_j = 1 \mid X_i = 0)$  depends on the degree of  $i$  and the degree of  $j$ .

The left plot shows for each node  $i$  a simulated estimate of

$$\frac{1}{d_i} \sum_{j:i \sim j} \mathbb{P}(X_j = 1 \mid X_i = 0), \quad (38)$$

the average fraction of time its neighbors are infected, given that  $i$  itself is healthy (blue markers). The plot shows that this quantity only mildly depends on the degree of  $i$ . The variation in this average of conditional probabilities is mainly explained by the variation in the degrees of the *neighbors* of  $i$ . Taking for each node  $i$  the ratio

$$\frac{\sum_{j:i \sim j} \mathbb{P}(X_j = 1 \mid X_i = 0)}{\sum_{j:i \sim j} \mathbb{P}(X_j = 1)}, \quad (39)$$

we get very little variation (red markers). It therefore seems quite reasonable to base heuristics on the assumption that

$$\frac{1}{d_i} \sum_{j:i \sim j} \mathbb{P}(X_j = 1 \mid X_i = 0) \approx \eta \cdot \frac{1}{d_i} \sum_{j:i \sim j} \mathbb{P}(X_j = 1) \quad (40)$$

for some constant  $0 < \eta < 1$  which does not depend on  $i$  and to try to estimate  $\eta$ . For each degree  $d$ , we also plotted the average of the conditional and of the unconditional probabilities,

$$\frac{1}{\#\{i : d_i = d\}} \sum_{i:d_i=d} \frac{1}{d} \sum_{j:i \sim j} \mathbb{P}(X_j = 1 \mid X_i = 0), \quad (41)$$

$$\frac{1}{\#\{i : d_i = d\}} \sum_{i:d_i=d} \frac{1}{d} \sum_{j:i \sim j} \mathbb{P}(X_j = 1) \quad (42)$$

and their ratio's (39) averaged over  $i$  (red). From the values on the yellow curve, we can reproduce an estimate of the size-biased infected fraction  $\tilde{\mu}/n$  by taking a weighted average:

$$\frac{\tilde{\mu}}{n} = \frac{1}{n} \sum_{d=1}^{n-1} \sum_{i:d_i=d} \frac{1}{d} \sum_{j:i \sim j} \mathbb{P}(X_j = 1). \quad (43)$$

Dependence of  $\mathbb{P}(X_j = 1 \mid X_i = 0)$  on the degree of  $j$  is visible in the right plot of Figure 13. Each blue marker now corresponds to a single ordered edge  $(i, j)$ . Dependence of  $\mathbb{P}(X_j = 1)$  on the degree of  $j$  has already been observed before, and here we see very similar patterns for the conditional probabilities  $\mathbb{P}(X_j = 1 \mid X_i = 0)$ . Averages of conditional and of unconditional probabilities are again given by the curves.

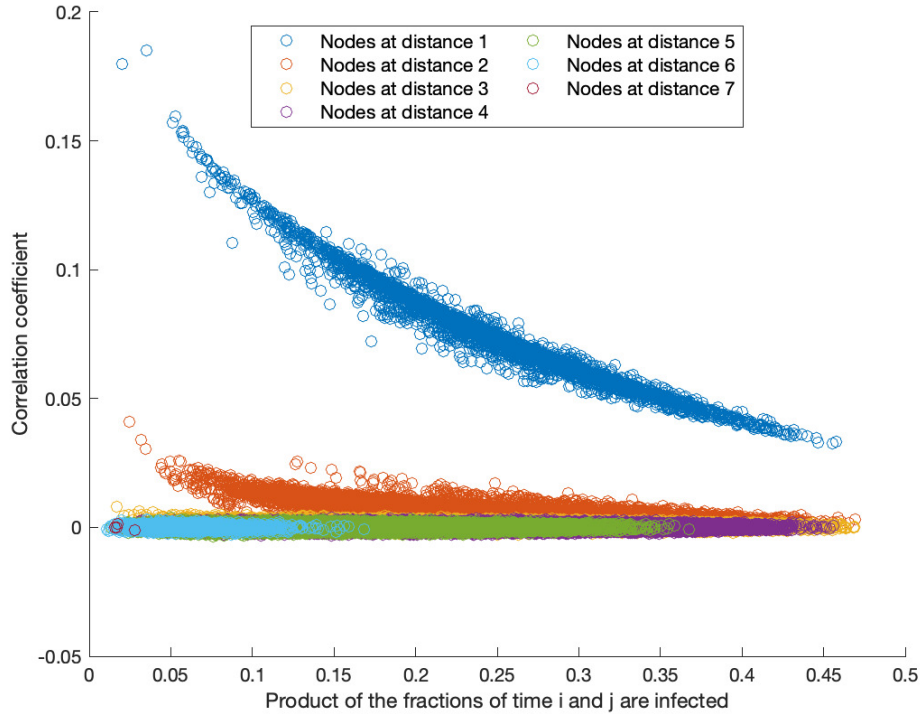


Figure 14: Correlations for each pair of nodes. The color indicates the distance in the graph.

## 4 Taking size-bias and neighbor correlations into account

The two types of systematic errors work in opposite directions. Ignoring the size-bias effect means that we underestimate the fraction of time neighbors of a random node  $i$  are infected. Then we also underestimate the rate at which  $i$  is infected. Eventually, this comes down to underestimation of the infected fraction  $\mu/n$  of the population.

On the other hand, neighbors of a healthy node are less likely to be infected. Ignoring this correlation means that we overestimate the rate at which  $i$  is infected, which eventually leads to overestimation of the infected fraction of the population.

The two errors might cancel sometimes, but in general this will not be the case, see for instance the smaller degrees in Figure 11. We therefore will propose heuristics to repair both errors. Presumably, nodes are still positively correlated if they are not direct neighbors. We again simulated the case  $n = 1000$ ,  $p = \log(n)/n$  and  $\lambda = 2$ . Figure 14 gives for each pair of nodes  $i$  and  $j$  the estimated correlation coefficient as a function of the product  $\mathbb{P}(X_i = 1)\mathbb{P}(X_j = 1)$ . The

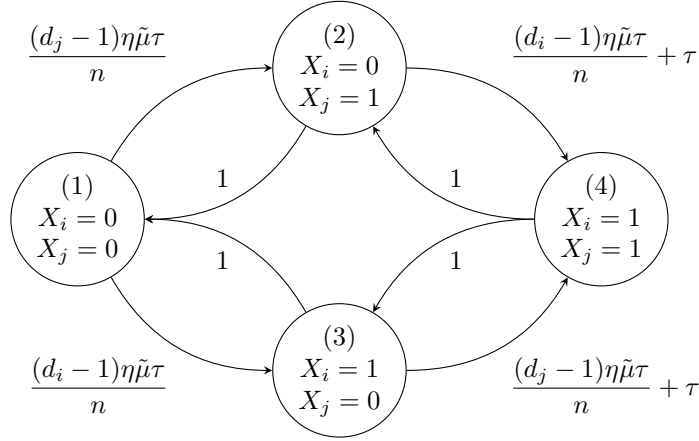


Figure 15: Transition diagram for infectious status of  $i$  and  $j$ . States are numbered (1), ..., (4).

color indicates the distance between  $i$  and  $j$  in the graph. Typically, if two nodes have high infection probabilities ( $\mathbb{P}(X_i = 1)\mathbb{P}(X_j = 1)$  large), then the distance between  $i$  and  $j$  is small. And finally, correlations rapidly decrease when the distance increases. Based on this last observation, we will design a heuristic which takes correlations between direct neighbors into account, but ignores correlations between other pairs of nodes.

Consider random nodes  $i$  and  $j$  which are neighbors and have degrees  $d_i \geq 1$  and  $d_j \geq 1$ . We make the following assumptions:

1. All neighbors of  $i$  and  $j$  (except  $i, j$  themselves) are infected the same fraction of time. We assume this fraction to be independent of  $d_i$  and  $d_j$ , and equal to the (unknown) size-biased infected fraction  $\tilde{\mu}/n$ :

$$\mathbb{P}(X_k = 1) = \tilde{\mu}/n, \quad \text{for } k \sim i \text{ or } k \sim j, k \neq i, j.$$

2. All these neighbors are assumed to be independent of each other.
3. There exists a constant  $\eta \in (0, 1)$  such that

- $\mathbb{P}(X_k = 1 \mid X_i = 0) = \eta\tilde{\mu}/n$  for each  $k \sim i, k \neq j$ .
- $\mathbb{P}(X_k = 1 \mid X_j = 0) = \eta\tilde{\mu}/n$  for each  $k \sim j, k \neq i$ .

Note that we do not use degrees other than the degrees of  $i$  and  $j$ . This causes the first assumption to be quite inaccurate for individual nodes, but it does keep the analysis feasible and the errors will mostly average out.

Under these assumptions, we are interested in the simultaneous evolution of nodes  $i$  and  $j$ . This evolution is described by a Markov chain on four states, with transition rates in the diagram in Figure 15.

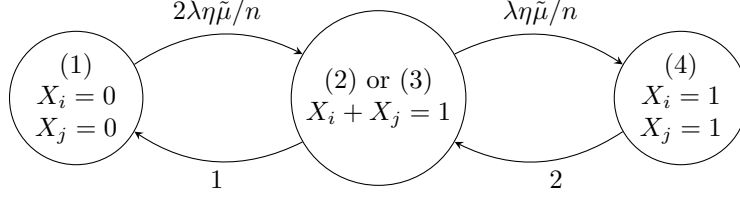


Figure 16: Transition diagram for infectious status of  $i$  and  $j$  as  $np \rightarrow \infty$

This Markov chain has a unique stationary distribution, which is found by solving the equations

$$\begin{cases} \mathbf{x}^T Q = \mathbf{0}^T, \\ \mathbf{x}^T \mathbf{1} = 1, \end{cases} \quad \mathbf{x}^T = (x_1 \quad x_2 \quad x_3 \quad x_4), \quad (44)$$

where  $\mathbf{0}$  and  $\mathbf{1}$  are the all zero and all one vector in  $\mathbb{R}^4$  and  $Q = (Q_{k,\ell})$  is the generator matrix:

$$Q = \begin{pmatrix} -\sum_{\ell \neq 1} Q_{1,\ell} & (d_j - 1)\eta\tilde{\mu}\tau/n & (d_i - 1)\eta\tilde{\mu}\tau/n & 0 \\ 1 & -\sum_{\ell \neq 2} Q_{2,\ell} & 0 & ((d_i - 1)\eta\tilde{\mu}\tau/n) + \tau \\ 1 & 0 & -\sum_{\ell \neq 3} Q_{3,\ell} & ((d_j - 1)\eta\tilde{\mu}\tau/n) + \tau \\ 0 & 1 & 1 & -\sum_{\ell \neq 4} Q_{4,\ell} \end{pmatrix}. \quad (45)$$

The matrix  $Q$  has rank 3 and the equations in (44) have a unique solution, giving  $x_1, \dots, x_4$  as functions of  $n, \tau, d_i, d_j, \eta$  and  $\tilde{\mu}$ . In principle these functions can be determined exactly. We will not do this, but we will show that in this system  $X_i$  and  $X_j$  have positive correlation, which vanishes if the degrees go to infinity. This agrees with conjectured and simulated behaviour of the contact process.

First we take a look at the Markov chain for  $np \rightarrow \infty$ . In this case, by the law of large numbers,  $(d_i - 1)/(np) \rightarrow 1$  and  $(d_j - 1)/(np) \rightarrow 1$  as  $n \rightarrow \infty$ . Since  $\tau = \lambda/(np)$  is of order  $(np)^{-1}$ , all rates to the right are of constant order and asymptotically equal to  $\lambda\eta\tilde{\mu}/n$ . By symmetry, states (2) and (3) will then have the same stationary probability. The Markov chain therefore asymptotically simplifies to the one in Figure 16. Solving for the stationary distribution of this system, we can easily find  $\mathbf{x}$  as well:

$$\mathbf{x}^T = \frac{1}{(1+c)^2} \cdot (1, c, c, c^2), \quad \text{where } c = \frac{\lambda\eta\tilde{\mu}}{n}. \quad (46)$$

We note that from this solution it follows that nodes  $i$  and  $j$  become independent as the degrees go to  $\infty$ :

$$\mathbb{P}(X_i = 0) \cdot \mathbb{P}(X_j = 0) = (x_1 + x_2)(x_1 + x_3) = \left( \frac{1+c}{(1+c)^2} \right)^2 = \mathbb{P}(X_i = X_j = 0). \quad (47)$$

Now consider the more complicated Markov chain of Figure 15. To avoid very awkward calculations, define

$$a = \frac{(d_i - 1)\eta\tilde{\mu}\tau}{n}, \quad b = \frac{(d_j - 1)\eta\tilde{\mu}\tau}{n}. \quad (48)$$

Since  $\tau > 0$ , the rate from  $X_i = 0$  to  $X_i = 1$  is at least  $a$ . Therefore,

$$\mathbb{P}(X_i = 0) = x_1 + x_2 < \frac{1}{1+a}, \quad \mathbb{P}(X_j = 0) = x_1 + x_3 < \frac{1}{1+b},$$

so that in particular there exist constants  $r_1, r_2 < 1$  for which  $x_1 + x_2 = r_1/(1+a)$  and  $x_1 + x_3 = r_2/(1+b)$ . Further, the detailed balance equation for state (1) yields  $(a+b)x_1 = x_2 + x_3$ , and hence

$$(2+a+b)x_1 = 2x_1 + x_2 + x_3 = \frac{r_1}{1+a} + \frac{r_2}{1+b}. \quad (49)$$

Solving this for  $x_1 = \mathbb{P}(X_i = X_j = 0)$ , we obtain

$$\mathbb{P}(X_i = X_j = 0) = \frac{r_1(1+b) + r_2(1+a)}{(1+a)(1+b)(2+a+b)} \quad (50)$$

$$> \frac{r_1 r_2}{(1+a)(1+b)} = \mathbb{P}(X_i = 0) \cdot \mathbb{P}(X_j = 0), \quad (51)$$

proving positive correlation for all choices of the parameters.

As noted, given the parameters  $n, \tau, d_i, d_j$ , we can determine the solution  $\mathbf{x}$ . However, this solution will still depend on the unknown  $\eta$  and  $\tilde{\mu}$ . To solve for these variables, we need additional equations.

So far,  $i$  and  $j$  have played the same role. But now we consider  $j$  to be a random neighbor of a randomly chosen node  $i$ . This is only possible if  $i$  has degree at least 1. In a connected graph, this is automatic. In an Erdős-Rényi graph with small  $p$ , it means that  $d_i$  has distribution  $\text{Bin}(n-1, p)$ , conditioned on being non-zero. The node  $j$  has the size-biased degree distribution  $d_j - 1 \sim \text{Bin}(n-2, p)$ , which is non-zero by definition. Consequently,  $j$  has the same degree distribution as all neighbors of  $i$  and  $j$  (except  $i$  itself). It therefore makes sense to approximate the expected fraction of time  $j$  is infected by the same  $\tilde{\mu}/n$ . Concretely, for each combination of  $d_i$  and  $d_j$ , we solve the system (44) for  $\mathbf{x}$ . In particular we get a different solution  $\mathbb{P}(X_j = 1) = x_2(d_i, d_j) + x_4(d_i, d_j)$  for each combination  $(d_i, d_j)$ . Then we take a weighted average according to the degree distributions of  $i$  and  $j$ . The resulting equation is

$$\frac{\tilde{\mu}}{n} = \sum_{d_i=1}^{n-1} \sum_{d_j=1}^{n-1} P^{(\geq 1)}(n, p, d_i) \tilde{P}(n, p, d_j) (x_2(d_i, d_j) + x_4(d_i, d_j)), \quad (52)$$

where  $P^{(\geq 1)}(n, p, d_i)$  and  $\tilde{P}(n, p, d_j)$  are the probabilities that  $i$  and  $j$  have degrees  $d_i$  and  $d_j$  respectively. That is,

$$P^{(\geq 1)}(n, p, d_i) = \mathbb{P}(D = d_i \mid D \geq 1), \quad D \sim \text{Bin}(n-1, p), \quad (53)$$

$$\tilde{P}(n, p, d_j) = \mathbb{P}(\tilde{D} = d_j), \quad \tilde{D} \sim 1 + \text{Bin}(n-2, p). \quad (54)$$

Of course these probabilities can be replaced by suitable approximations for large  $n$  or by graph-based estimates (see Section 5).

Another equation is obtained by considering conditional probabilities. Since  $\mathbb{P}(X_j = 1 \mid X_i = 0)$  hardly depends on the degree of  $i$  (supported by Figure 13), we can assume this conditional probability to be equal to  $\eta\tilde{\mu}$ . In terms of  $\mathbf{x}$ , we have  $\mathbb{P}(X_j = 1 \mid X_i = 0) = x_2/(x_1 + x_2)$ . Proceeding along the same lines as above, we obtain

$$\frac{\eta\tilde{\mu}}{n} = \sum_{d_i=1}^{n-1} \sum_{d_j=1}^{n-1} P^{(\geq 1)}(n, p, d_i) \tilde{P}(n, p, d_j) \frac{x_2(d_i, d_j)}{x_1(d_i, d_j) + x_2(d_i, d_j)}. \quad (55)$$

If all parameters of the process are given, the equations (44), (52) and (55) can be solved to find  $\eta$  and  $\tilde{\mu}$ . Finding exact expressions is a tall order, but an iterative numerical procedure gives satisfactory results.

The solutions for  $\eta$  and  $\tilde{\mu}$  only depend (in a complicated way) on the process parameters  $n$ ,  $p$  and  $\tau$ . Once they have been determined, we can plug them into  $\mathbf{x}$ , which will then be a function of the same parameters and the degrees  $d_i$  and  $d_j$ . This allows to compute an estimate for  $\mu$  in the same fashion, by using that  $\mathbb{P}(X_i = 1) = x_3 + x_4$  and taking a weighed average similar to (52). This time, we first pick a random node  $i$ . If it has degree 0, it will not contribute to  $\mu$  (it quickly heals and never gets infected again). If it has degree  $\geq 1$ , we let  $j$  be a random neighbor of  $i$ . The estimate for  $\mu$  then is

$$\frac{\mu}{n} = \sum_{d_i=1}^{n-1} \sum_{d_j=1}^{n-1} P(n, p, d_i) \tilde{P}(n, p, d_j) (x_3(d_i, d_j) + x_4(d_i, d_j)), \quad (56)$$

with

$$P(n, p, d_i) = \mathbb{P}(D = d_i), \quad D \sim \text{Bin}(n-1, p). \quad (57)$$

The subtle difference with (52) and (55) is that now  $i$  is not conditioned to have degree  $\geq 1$ , though still degree 0 does not contribute to the sum.

The resulting equations for  $\tilde{\mu}$  and  $\mu$  can be seen as a more sophisticated version of the Heterogeneous Mean Field method ((32) and (33)). It takes size-bias effects and correlations simultaneously into account. We now obtain a new annealed heuristic for predicting  $\mu$  as a function of  $n$ ,  $p$  and  $\tau$ :

**Heuristic 5 (Annealed).** *Let  $G = (V, E)$  be an Erdős-Rényi graph with parameters  $n$  and  $p$ . Consider the contact process on  $G$  with infection rate  $\tau$ . For each  $1 \leq d_i, d_j \leq n-1$ , let  $\mathbf{x}(d_i, d_j)$  be the solution of (44), which depends on the unknowns  $\tilde{\mu}$  and  $\eta$ . Solve (52) and (55) for  $\tilde{\mu}$  and  $\eta$  and substitute the solutions in  $\mathbf{x}(d_i, d_j)$ . Finally, take the weighted average (56) to obtain a prediction for  $\mu$ .*

Before turning to the numerical results, we wrap up our discussion on asymptotics for  $np \rightarrow \infty$ . The degree distributions of  $d_i$  and  $d_j$  concentrate around

their expectations, and  $\mathbf{x}$  becomes independent of the degrees as in (46). The equations (52) and (55) become

$$\frac{\tilde{\mu}}{n} = x_2 + x_4 = \frac{c + c^2}{(1 + c)^2} = \frac{c}{1 + c} \quad (58)$$

$$\frac{\eta \tilde{\mu}}{n} = \frac{x_2}{x_1 + x_2} = \frac{c/(1 + c)^2}{(1 + c)/(1 + c)^2} = \frac{c}{1 + c}, \quad (59)$$

and solving them gives

$$\tilde{\mu} = \frac{\lambda - 1}{\lambda} n, \quad \eta = 1. \quad (60)$$

Since  $x_2 = x_3$  in this case, we also get  $\mu = \tilde{\mu}$ . The conclusion is that according to Heuristic 5, both the size-bias effect and the correlations vanish if the degrees go to infinity. This conclusion is consistent with simulations and intuition. Also note that the asymptotic prediction for  $\mu$  agrees with Heuristic 1, which can be seen as a small sanity check. Finally, no solution exists for  $\lambda < 1$ , reflecting the fact that the process has no metastable behaviour in this case.

#### 4.1 Quenched variants

Heuristic 5 can be reinforced if information about the graph is available. In particular, we can replace  $P(n, p, d)$ ,  $P^{(\geq 1)}(n, p, d)$  and  $\tilde{P}(n, p, d)$  with graph-based estimates. We only have to do this for  $d \geq 1$ . We have the following quenched variants of Heuristic 5:

**Heuristic 5** (Quenched variants). (a) *Estimate  $p$  by the number of edges  $m$  in the graph:  $\hat{p} = \frac{2m}{n(n-1)}$  and use  $P(n, \hat{p}, d)$ ,  $P^{(\geq 1)}(n, \hat{p}, d)$  and  $\tilde{P}(n, \hat{p}, d)$ .*

(b) *Estimate probabilities by true degree frequencies in the graph:*

$$P(n, p, d) = \frac{\#\{i : d_i = d\}}{n} = \frac{1}{n} \sum_{i=1}^n \mathbf{1}\{d_i = d\}, \quad (61)$$

$$P^{(\geq 1)}(n, p, d) = \frac{\#\{i : d_i = d\}}{\#\{i : d_i \geq 1\}} = \frac{\sum_{i=1}^n \mathbf{1}\{d_i = d\}}{\sum_{i=1}^n \mathbf{1}\{d_i \geq 1\}}, \quad (62)$$

$$\tilde{P}(n, p, d) = \frac{1}{\#\{i : d_i \geq 1\}} \sum_{i=1, d_i \geq 1}^n \frac{1}{d_i} \sum_{j \sim i} \mathbf{1}\{d_j = d\}. \quad (63)$$

(c) *Estimate products of probabilities by true frequencies in the graph:*

$$P(n, p, d) \cdot \tilde{P}(n, p, e) = \frac{1}{n} \sum_{i=1}^n \sum_{j \sim i} \frac{\mathbf{1}\{d_i = d, d_j = e\}}{d}, \quad (64)$$

$$P^{(\geq 1)}(n, p, d) \cdot \tilde{P}(n, p, e) = \frac{1}{\#\{i : d_i \geq 1\}} \sum_{i=1}^n \sum_{j \sim i} \frac{\mathbf{1}\{d_i = d, d_j = e\}}{d}. \quad (65)$$

As in NIMFA, one could even use the full adjacency matrix of the graph, but computations would be more complicated.



## 5 Heuristic 5, numerical results

In this section we review the performance of annealed and quenched variants of Heuristic 5. For  $p$  equal to the connectivity threshold  $\log(n)/n$ , Heuristics 2 and 3 are already very good (Figures 8 and 9). Nevertheless, Heuristic 5 seems to give a small improvement here. We will not discuss this in detail.

The real test case is the very sparse Erdős-Rényi graph with  $p$  significantly below the connectivity threshold. In this case all heuristics which do not take into account correlations fail to accurately predict. This is the case for NIMFA and HMF, but in this sparse regime it also applies to Heuristics 2 and 3. We will demonstrate how Heuristic 5 can be used to get accurate predictions in this regime (Section 5.1).

Heuristic 5 does not only give accurate predictions for the infected fraction of the population. As a bonus, it can also be exploited to obtain estimates for other quantities like correlations between nodes (Section 5.2).

### 5.1 Estimation in sparse graphs, the regime $p = c/n$

The effect of correlations and size-bias becomes more important when degrees in the graph are smaller. So far we mostly looked at Erdős-Rényi graphs with  $p$  close to or above the connectivity threshold. In these cases, variants of Heuristic 2 still do reasonably well. Below the connectivity threshold, the picture changes.

In the left plot of Figure 17, we compare all annealed heuristics for Erdős-Rényi graphs of 1000 nodes with  $p = c/n$  and the average degree  $c$  ranging from 1.1 to 7 ( $\approx \log(n)$ ). In all cases,  $\lambda = 2$ . For each parameter combination and heuristic, an average of simulations is compared with the corresponding predictions. The Heterogeneous Mean Field method substantially overestimates the infected fraction in these sparse graphs. Our new Heuristic 5 is more accurate than Heuristic 2a, but still struggles when the degrees get really small.

This point is once again illustrated by Figure 17 (right), where we zoom in on the errors for 100 replications of the case  $c = 2$ . Quenched heuristics have a smaller error margin, and variants of Heuristic 5 have the smallest bias. But they still do overestimate the infected fraction in these very sparse graphs. One reason is that a substantial fraction of the nodes is not in the largest component.

For  $p = c/n$ ,  $c > 1$ , the graph disconnects and there will be a unique giant component. This giant component has size about  $y \cdot n$ , with  $y$  the largest solution of  $1 - y = e^{-cy}$ , see [30]. All other components will be much smaller, of size at most logarithmic in  $n$ . In these small components the infection quickly disappears. The metastable infected fraction of the population therefore will be less than the size of the giant component. The simulation in Figure 17 confirms this, but none of the heuristics captures this effect.

Another feature of these very sparse graphs is that the degree distribution inside the giant will differ from the degree distribution in the whole graph. For instance, isolated nodes never appear in the giant. Similarly, size-biased degree distributions inside and outside the giant component are different. In general, degrees inside the giant component will be larger.

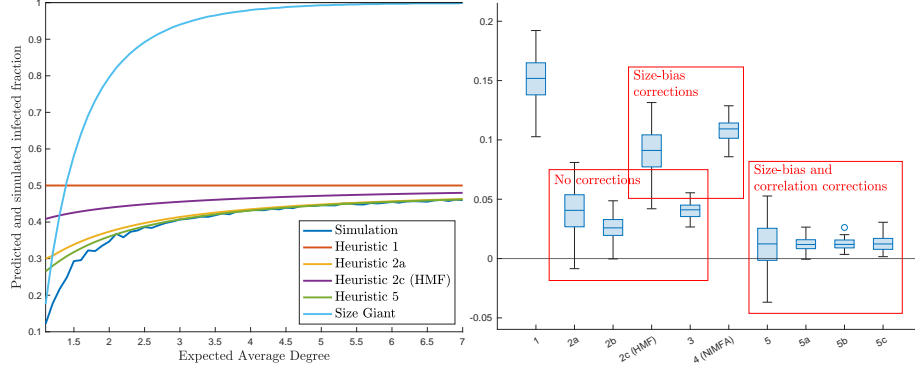


Figure 17: Sparse Erdős-Rényi graphs. Left: simulation compared to annealed heuristics. Right: prediction errors for all heuristics in Erdős-Rényi graphs with average degree 2.

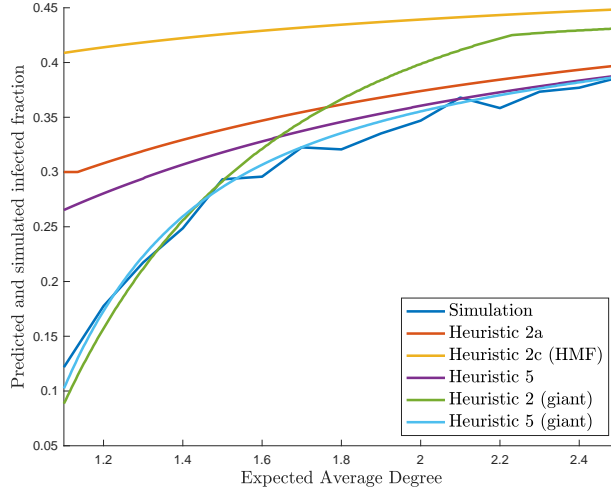


Figure 18: Most heuristics are wrong in very sparse Erdős-Rényi graphs. One should take the degree distribution of the giant and apply size-bias and correlation corrections (light blue).

Our implementations of Heuristic 5 so far do not account for these properties of subcritical Erdős-Rényi graphs. For the degree distribution they just take the binomials which apply to the whole graph. However, for small  $c$ , one should restrict the analysis to the giant and use the corresponding degree distributions. The calculation of these distributions is discussed in Appendix A. Heuristic 5 can then be used to predict the infected fraction within the giant. After rescaling by the size of the giant, we obtain estimates for  $\mu/n$  in the Erdős-Rényi graph. Figure 18 shows that this gives pretty accurate results. It also shows that it is insufficient to just apply Heuristic 2 inside the giant. Correlations and size-bias have to be taken into account as well.

In a similar fashion quenched heuristics can be applied to the giant component. An illustration is given in Figure 4, where the quenched method actually is Heuristic 5a applied to the giant. These quenched versions also turn out to give very accurate estimates.

The analysis of the giant serves as a test case for graphs with other degree distributions. Since our methods work quite well in the giant, we expect them to apply to graphs with other degree distributions as well. Which features of the graph are essential to make the methods work requires further research. We expect that the methods are less suitable for graphs with a high variation in degrees (like power-law degree distributions) and for graphs which locally do not look like a tree (like grids). Graphs for which we do expect good results include the random regular graph.

## 5.2 Estimating per-node infected fractions, correlations and the total variance

The ideas behind Heuristic 5 give more information than just a prediction for  $\mu$ . After solving all equations, we know  $\mathbf{x}(d_i, d_j)$  for all combinations of  $d_i$  and  $d_j$ . This means that we can make degree-dependent predictions. For instance, to estimate the fraction of time a random node of degree  $d$  is infected, take  $d_i = d$  and average over  $d_j$  (cf. (56)). Similarly, we can estimate conditional probabilities.

For illustration, we simulated the process on an Erdős-Rényi graph on  $n = 10^4$  nodes with  $p = \log(n)/n$  and  $\lambda = 2$ . See Figure 19. In blue we plotted the infection probabilities  $\mathbb{P}(X_j = 1)$  and  $\mathbb{P}(X_j = 1 \mid X_i = 0)$  for pairs of nodes  $(i, j)$  as functions of their degrees. All this is essentially the same as Figure 13, but now we can predict these quantities as follows.

Let  $i$  and  $j$  be neighboring nodes. First we solve for  $\mathbf{x}(d_i, d_j)$  as in Heuristic 5. An approximation for  $\mathbb{P}(X_j = 1 \mid X_i = 0)$  is  $x_2/(x_1 + x_2)$ . Fixing  $d_i$  and taking a weighted average over all values of  $d_j$  gives a prediction for  $\mathbb{P}(X_j = 1 \mid X_i = 0)$  as function of  $d_i$ . Similarly, we get predictions as function of  $d_j$ . These predictions are as in (55), but now only summing over  $d_j$  or only over  $d_i$  respectively. For the unconditional probabilities  $\mathbb{P}(X_j = 1)$ , the procedure is analogous, but now using (52). In fact, by looking at pairs, we are predicting a version of a size-biased distribution here. Similar methods can be used to predict the infected

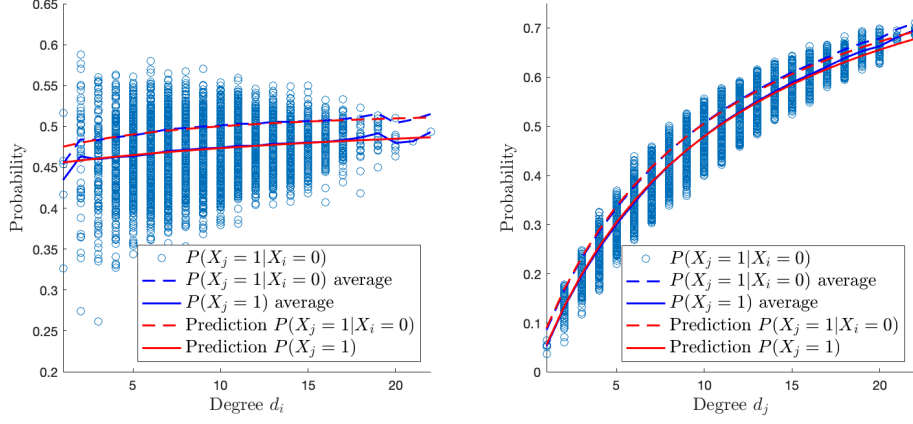


Figure 19: Infection probabilities and conditional infection probabilities for pairs  $(i, j)$  with predictions. Left: averaged over neighbors of  $i$  and as function of  $d_i$ . Right: as function of  $d_j$ .

fraction of time for a random node with degree  $d_i$  using (56) and only summing over  $d_j$ .

Another feature of interest are correlations between neighbors. For an edge  $(i, j)$  with degrees  $d_i$  and  $d_j$ , we can again solve for  $\mathbf{x}(d_i, d_j)$  and then predict the correlation coefficient of  $i$  and  $j$  by the formula

$$\rho(X_i, X_j) \approx \frac{x_4 - (x_3 + x_4) \cdot (x_2 + x_4)}{\sqrt{(x_3 + x_4)(1 - (x_3 + x_4)) \cdot (x_2 + x_4)(1 - (x_2 + x_4))}}, \quad (66)$$

based on (36). Plotting this against

$$\mathbb{P}(X_i = 1) \cdot \mathbb{P}(X_j = 1) \approx (x_3 + x_4) \cdot (x_2 + x_4) \quad (67)$$

gives Figure 20. The left hand sides of (66) and (67) are simulated, the right hand sides are predictions. For each combination of degrees  $d_i$  and  $d_j$ , there is one predicted point, plotted as a red marker. The size of the marker is proportional to the probability of the degree pair  $(d_i, d_j)$ . We see that correlations are maybe slightly underestimated for the less likely degree combinations. This could be explained by the fact that Heuristic 5 ignores correlations at distance 2 and larger.

One could wonder if we can use these correlation estimates to obtain predictions for the variance of the number of infected nodes. We have

$$\text{Var} \left( \sum_{i=1}^n X_i \right) = \sum_{i=1}^n \text{Var}(X_i) + 2 \sum_{i \neq j} \text{Cov}(X_i, X_j). \quad (68)$$

For instance, in the complete graph expectation and variances are known:  $\mathbb{E}[X_i] =$

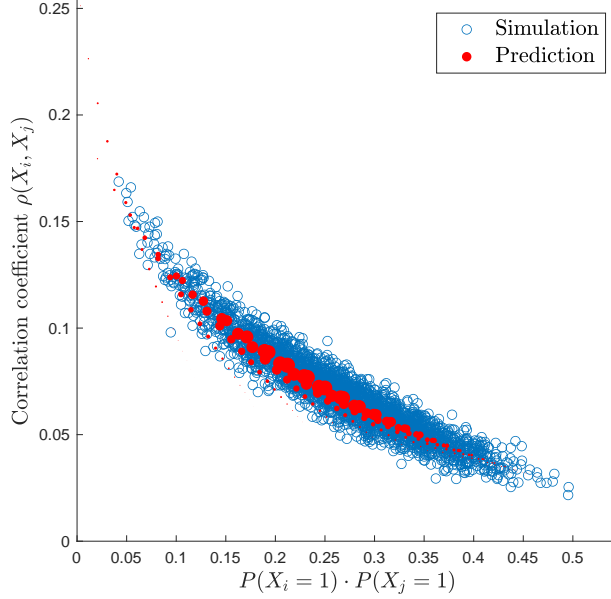


Figure 20: Simulated and predicted correlations.

$1 - \frac{1}{\lambda}$ ,  $\text{Var}(X_i) = \frac{1}{\lambda}(1 - \frac{1}{\lambda})$  and  $\text{Var}(\sum X_i) = \frac{n}{\lambda}$ . Substituting in (68) gives

$$\frac{n}{\lambda} = \frac{n}{\lambda}(1 - \frac{1}{\lambda}) + n(n-1)\text{Cov}(X_1, X_2), \quad (69)$$

So we can compute the covariances as well to find  $\text{Cov}(X_1, X_2) \sim 1/(n\lambda^2)$ . This means that pair covariances are small compared to node variances, but the sum of covariances significantly contributes to the total variance.

In the Erdős-Rényi graph, we can estimate  $\mu = \sum \mathbb{E}[X_i]$  as in (56). Similarly, we estimate the sum of variances  $\sum \text{Var}(X_i) = \sum \mathbb{E}[X_i^2] - \mathbb{E}[X_i]^2$  by taking a weighted average of degree-dependent predictions.

For covariances of neighbors, we have degree-dependent predictions  $\text{Cov}(d_i, d_j)$  as well in the numerator of 66. This can be used to predict

$$2 \sum_{i \sim j} \text{Cov}(X_i, X_j) \approx pn(n-1) \sum_{d_i=1}^{n-1} \sum_{d_j=1}^{n-1} \tilde{P}(n, p, d_i) \tilde{P}(n, p, d_j) \text{Cov}(d_i, d_j). \quad (70)$$

The right hand side is twice the expected number of edges, multiplied by the predicted covariance for a randomly chosen edge. A subtlety to be noted here is the weighting: if we pick a random edge, then both endpoints have the size-biased degree distribution.

What is still missing to predict the total variance in (68) are covariances for pairs of non-neighboring nodes. Figure 21 shows simulations ( $p = \log(n)/n$ ,  $\lambda =$

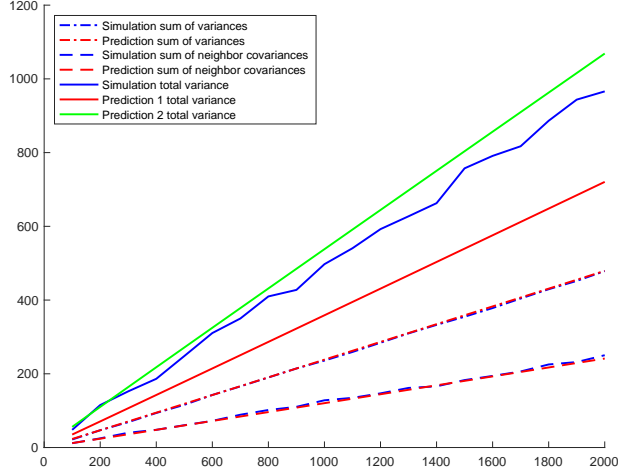


Figure 21: Simulations and predictions of variances and covariances.

2) and predictions for the terms

$$\sum_i \text{Var}(X_i), \quad 2 \sum_{i \sim j} \text{Cov}(X_i, X_j). \quad (71)$$

Both terms are predicted quite accurately. However, the sum of these two (solid red in the figure) turns out to be a bad prediction for the total variance, which was simulated as well. This means that we can not ignore correlations between nodes at mutual distance 2 or larger. The covariances  $\text{Cov}(X_i, X_j)$  for  $i \not\sim j$  are much smaller (cf. Figure 14), but the number of pairs is much larger, making the sum a significant contribution to the total variance. Since Heuristic 5 is based on analysis of direct neighbors, it falls short to predict the total variance.

There is however another way to predict the total variance. In equilibrium, the total healing rate is equal to  $\mu n$ . By definition of equilibrium, this is equal to the total infection rate. For a uniformly at random selected set of  $\mu n$  nodes, we expect  $p\mu(1-\mu)n^2$  edges to its complement. The set of infected nodes is *not* a uniform selection (e.g. high degrees are overrepresented). Still, if the number of infected  $k$  is close to equilibrium, we can assume that the number of edges to the complement is proportional  $k(n-k)$ . In equilibrium ( $k = \mu n$ ), the total infection rate is  $\tilde{p}\tau\mu(1-\mu)n^2$ , where  $\tilde{p}$  is a conditional edge probability given that we consider a healthy and an infected node. This gives the equilibrium equation

$$\mu n = \tilde{p}\tau\mu(1-\mu)n^2, \quad (72)$$

so that  $\tilde{p}\tau$  is equal to the reciprocal of the number  $(1-\mu)n$  of healthy nodes in equilibrium. Note that this is consistent with the complete graph, when  $p = \tilde{p} = 1$ .

Now suppose the number of infected deviates a bit from equilibrium and is equal to  $k = \mu n + d$ . The ratio of total infection and total healing rate is then given by

$$\frac{\tilde{p}\tau(\mu n + d)((1 - \mu)n - d)}{\mu n + d} = 1 - \frac{d}{(1 - \mu)n}. \quad (73)$$

In this formula, we see a drift towards the equilibrium  $\mu n$ . This type of drift is known to lead to a Gaussian metastable distribution with variance  $(1 - \mu)n$ , see [1]. Since we have an estimate for  $\mu$ , we have an estimate for the variance as well, which is added to the plot in Figure 21 (solid green). This improves the prediction based on Heuristic 5, but is still biased. A better understanding of correlations of non-neighboring nodes will be needed to get more accurate variance estimates.

## A Degrees in the giant component

### A.1 Degree distribution in the giant component

Here we discuss the degree distribution in the giant component of a sparse Erdős-Rényi graph with edge probability  $p = c/n$ . Suppose that the graph has been created on  $n - 1$  nodes and that there is a giant component  $C$  of size  $y \cdot (n - 1)$  for some  $0 < y < 1$ . Add the last node to the graph, and connect it to other nodes with probability  $p$  independently. To be consistent, the probability that this node does not end up in the giant component has to be close to  $1 - y$ . This gives the equation

$$1 - y = (1 - p)^{(n-1)y} \sim e^{-cy}. \quad (74)$$

Indeed it can be shown rigorously that the size  $|C|/n$  of the giant is equal to the largest solution to this equation [30], at least asymptotically.

The degree distributions inside and outside the giant can be calculated in the same way. Create all edges between the first  $n - 1$  nodes, and suppose the giant in this graph has size  $C$ . Add the final node  $v$ . The probability that  $v$  has degree  $k$  and does not end up in the giant is

$$\mathbb{P}(D = k, v \notin C) = (1 - p)^{|C|} \cdot \binom{n - |C|}{k} p^k (1 - p)^{n - |C| - k - 1}. \quad (75)$$

In this expression  $|C|$  is a random variable as well. We can approximate the degree distribution of an arbitrary node by substituting  $y \cdot n$  for  $|C|$ . Further, we assume that  $k$  is small compared to  $n$ , to obtain

$$\mathbb{P}(D = k, v \notin C) \sim \frac{(c(1 - y))^k}{k!} e^{-c}. \quad (76)$$

This gives us

$$\mathbb{P}(D = k, v \in C) = \mathbb{P}(D = k) - \mathbb{P}(D = k, v \notin C) \quad (77)$$

$$\sim \frac{(1 - (1 - y)^k)c^k}{k!} e^{-c}, \quad (78)$$

and leads to the conditional probability

$$\mathbb{P}(D = k \mid v \in C) = \frac{\mathbb{P}(D = k, v \in C)}{\mathbb{P}(v \in C)} \quad (79)$$

$$\sim \frac{(1 - (1 - y)^k)c^k}{yk!} e^{-c}. \quad (80)$$

Now we can as well find an (asymptotic) estimate for the expected degree in the giant:

$$\begin{aligned} \mathbb{E}[D \mid v \in C] &= \sum_{k=1}^{\infty} \frac{k(1 - (1 - y)^k)c^k}{yk!} e^{-c} \\ &= \frac{e^{-c}}{y} \sum_{k=0}^{\infty} \frac{(1 - (1 - y)^{k+1})c^{k+1}}{k!} \\ &= \frac{e^{-c}}{y} (ce^c - (1 - y)ce^{(1-y)c}) \\ &= \frac{c}{y} (1 - e^{-2cy}) = \frac{c}{y} (1 - (1 - y)^2) = c(2 - y). \end{aligned}$$

If the expected degree  $c$  is close to 1, then the expected degree in the giant is close to 2 (the minimum needed for connectedness). If  $c$  is large, then  $y \approx 1$  and the expected degree inside the giant is approximately the same as the expected degree in the whole graph. This makes sense, since there is (almost) nothing outside the giant.

## A.2 Size-bias distribution in the giant component

Here we calculate the size-bias degree distribution in the giant component. Let  $u$  be an arbitrary node in the giant and let  $v$  be a random neighbor of  $u$ . We are interested in the degree distribution of  $v$ , which is the size-bias distribution inside the giant.

$$\mathbb{P}(d(v) = k \mid v \leftrightarrow u, u \in C) = \frac{\mathbb{P}(d(v) = k, v \leftrightarrow u, u \in C)}{\mathbb{P}(v \leftrightarrow u, u \in C)}. \quad (81)$$

Observe that

$$\mathbb{P}(v \leftrightarrow u, u \notin C) = \mathbb{P}(v \leftrightarrow u) \cdot \mathbb{P}(u \notin C \mid v \leftrightarrow u) = p \cdot (1 - p)^{2|C|} \quad (82)$$

$$\sim p \cdot e^{-2cy}. \quad (83)$$



Therefore

$$\mathbb{P}(v \leftrightarrow u, u \in C) = p \left(1 - (1-p)^{2|C|}\right) \sim p(1 - e^{-2cy}). \quad (84)$$

Moreover, for  $1 \leq k \ll n$  we have

$$\mathbb{P}(d(v) = k, v \leftrightarrow u, u \notin C) = p \cdot (1-p)^{2|C|} \cdot \binom{n-|C|-2}{k-1} p^{k-1} (1-p)^{n-|C|-k-1} \quad (85)$$

$$\sim \frac{(1-y)^{k-1} n^{k-1}}{(k-1)!} p^k e^{-c-cy} \quad (86)$$

$$= \frac{c^k \cdot (1-y)^k}{n(k-1)!} e^{-c}. \quad (87)$$

We further need that

$$\mathbb{P}(d(v) = k, v \leftrightarrow u) = p \cdot \mathbb{P}(\text{Bin}(n-2, p) = k-1) \quad (88)$$

$$= \binom{n-2}{k-1} p^k (1-p)^{n-k-1} \quad (89)$$

$$\sim \frac{n^{k-1} p^k}{(k-1)!} e^{-c} = \frac{c^k e^{-c}}{n(k-1)!}. \quad (90)$$

It now follows that

$$\mathbb{P}(d(v) = k, v \leftrightarrow u, u \in C) = \mathbb{P}(d(v) = k, v \leftrightarrow u) - \mathbb{P}(d(v) = k, v \leftrightarrow u, u \notin C) \quad (91)$$

$$= \binom{n-2}{k-1} p^k (1-p)^{n-k-1} - \binom{n-|C|-2}{k-1} \cdot p^k \cdot (1-p)^{n-k-1+|C|} \quad (92)$$

$$\sim \frac{c^k e^{-c}}{n(k-1)!} (1 - (1-y)^k), \quad (93)$$

which leads to the following size-bias distribution in the giant:

$$\mathbb{P}(d(v) = k \mid v \leftrightarrow u, u \in C) = \frac{p^{k-1} (1-p)^{n-k-1} \left( \binom{n-2}{k-1} - \binom{n-|C|-2}{k-1} \cdot (1-p)^{|C|} \right)}{1 - (1-p)^{2|C|}}, \quad (94)$$

The asymptotic approximation is

$$\mathbb{P}(d(v) = k \mid v \leftrightarrow u, u \in C) \sim \frac{p^{k-1} e^{-c} (n^{k-1} - ((1-y)n)^{k-1} \cdot e^{-cy})}{(k-1)! \cdot (1 - e^{-2cy})} \quad (95)$$

$$= \frac{c^{k-1} e^{-c} (1 - (1-y)^k)}{(k-1)! \cdot (1 - e^{-2cy})}. \quad (96)$$

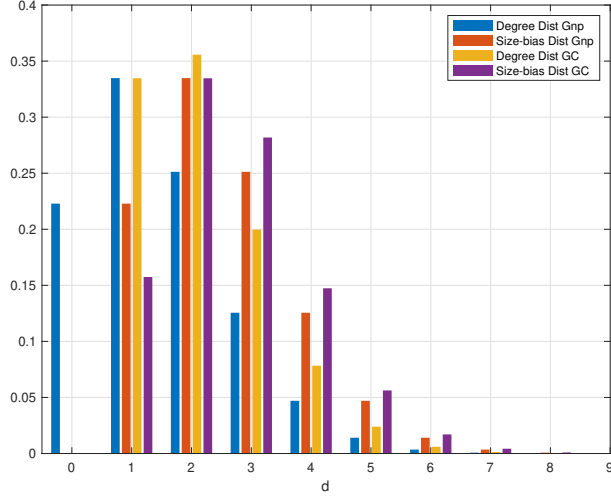


Figure 22: Four different degree distributions for  $G_{n,p}$  with  $p = \frac{3}{2n}$ .

One can check that this sums up to 1.

The degree distributions in the entire graph, in the giant component and their size-biased versions are all different in the sparse regime. See Figure 22. If the degrees go to infinity, these differences will be negligible.

## References

- [1] O. S. Awolude, E. Cator, and H. Don. Random walks on  $\mathbb{Z}$  with metastable gaussian distribution caused by linear drift with application to the contact process on the complete graph, 2023.
- [2] Shankar Bhamidi, Danny Nam, Oanh Nguyen, and Allan Sly. Survival and extinction of epidemics on random graphs with general degree. *Ann. Probab.*, 49(1):244–286, 2021.
- [3] Béla Bollobás. *Random graphs*. Academic Press, Inc. [Harcourt Brace Jovanovich, Publishers], London, 1985.
- [4] E. Cator and H. Don. Explicit bounds for critical infection rates and expected extinction times of the contact process on finite random graphs. *Bernoulli*, 27(3):1556–1582, 2021.
- [5] E. Cator and P. Van Mieghem. Second-order mean-field susceptible-infected-susceptible epidemic threshold. *Phys. Rev. E*, 85:056111, May 2012.

- [6] E. Cator and P. Van Mieghem. Susceptible-infected-susceptible epidemics on the complete graph and the star graph: Exact analysis. *Phys. Rev. E*, 87:012811, Jan 2013.
- [7] E. Cator and P. Van Mieghem. Nodal infection in markovian susceptible-infected-susceptible and susceptible-infected-removed epidemics on networks are non-negatively correlated. *Phys. Rev. E*, 89:052802, May 2014.
- [8] Odo Diekmann, Hans Heesterbeek, and Tom Britton. *Mathematical tools for understanding infectious disease dynamics*. Princeton Series in Theoretical and Computational Biology. Princeton University Press, Princeton, NJ, 2013.
- [9] Peter Donnelly. The correlation structure of epidemic models. *Mathematical Biosciences*, 117(1):49–75, 1993.
- [10] Richard Durrett and Xiu Fang Liu. The contact process on a finite set. *Ann. Probab.*, 16(3):1158–1173, 1988.
- [11] P. Erdős and A. Rényi. On random graphs. I. *Publ. Math. Debrecen*, 6:290–297, 1959.
- [12] P. Erdős and A. Rényi. On the evolution of random graphs. *Magyar Tud. Akad. Mat. Kutató Int. Közl.*, 5:17–61, 1960.
- [13] A. Ganesh, L. Massoulie, and D. Towsley. The effect of network topology on the spread of epidemics. In *Proceedings IEEE 24th Annual Joint Conference of the IEEE Computer and Communications Societies.*, volume 2, pages 1455–1466 vol. 2, 2005.
- [14] E. N. Gilbert. Random graphs. *Ann. Math. Statist.*, 30:1141–1144, 1959.
- [15] James P. Gleeson. High-accuracy approximation of binary-state dynamics on networks. *Phys. Rev. Lett.*, 107:068701, Aug 2011.
- [16] T. E. Harris. Contact interactions on a lattice. *Ann. Probability*, 2:969–988, 1974.
- [17] Xiangying Huang and Rick Durrett. The contact process on random graphs and Galton Watson trees. *ALEA Lat. Am. J. Probab. Math. Stat.*, 17(1):159–182, 2020.
- [18] J.O. Kephart and S.R. White. Directed-graph epidemiological models of computer viruses. In *Proceedings. 1991 IEEE Computer Society Symposium on Research in Security and Privacy*, pages 343–359, 1991.
- [19] Thomas M. Liggett. Multiple transition points for the contact process on the binary tree. *Ann. Probab.*, 24(4):1675–1710, 1996.

- [20] Thomas M. Liggett. *Stochastic interacting systems: contact, voter and exclusion processes*, volume 324 of *Grundlehren der mathematischen Wissenschaften [Fundamental Principles of Mathematical Sciences]*. Springer-Verlag, Berlin, 1999.
- [21] Cristopher Moore and M. E. J. Newman. Epidemics and percolation in small-world networks. *Phys. Rev. E*, 61:5678–5682, May 2000.
- [22] T. S. Mountford. A metastable result for the finite multidimensional contact process. *Canad. Math. Bull.*, 36(2):216–226, 1993.
- [23] Thomas Mountford, Daniel Valesin, and Qiang Yao. Metastable densities for the contact process on power law random graphs. *Electron. J. Probab.*, 18:No. 103, 36, 2013.
- [24] Jean-Christophe Mourrat and Daniel Valesin. Phase transition of the contact process on random regular graphs. *Electron. J. Probab.*, 21:Paper No. 31, 17, 2016.
- [25] World Health Organization. *From emergency response to long-term COVID-19 disease management: sustaining gains made during the COVID-19 pandemic*, volume WHO/WHE/SPP/2023.1. WHO Geneva, 2023.
- [26] Romualdo Pastor-Satorras, Claudio Castellano, Piet Van Mieghem, and Alessandro Vespignani. Epidemic processes in complex networks. *Rev. Modern Phys.*, 87(3):925–979, 2015.
- [27] Romualdo Pastor-Satorras and Alessandro Vespignani. Epidemic dynamics and endemic states in complex networks [j]. *Physical review. E, Statistical, nonlinear, and soft matter physics*, 63:066117, 07 2001.
- [28] Robin Pemantle. The contact process on trees. *Ann. Probab.*, 20(4):2089–2116, 1992.
- [29] Alan Stacey. The contact process on finite homogeneous trees. *Probab. Theory Related Fields*, 121(4):551–576, 2001.
- [30] Remco van der Hofstad. *Random graphs and complex networks. Vol. 1*, volume [43] of *Cambridge Series in Statistical and Probabilistic Mathematics*. Cambridge University Press, Cambridge, 2017.
- [31] Piet Van Mieghem, Jasmina Omic, and Robert Kooij. Virus spread in networks. *IEEE/ACM Transactions on Networking*, 17(1):1–14, 2009.
- [32] Yang Wang, D. Chakrabarti, Chenxi Wang, and C. Faloutsos. Epidemic spreading in real networks: an eigenvalue viewpoint. In *22nd International Symposium on Reliable Distributed Systems, 2003. Proceedings.*, pages 25–34, 2003.